Contrib Mineral Petrol (1989) 103:434–451

Contributions to Mineralogy and Petrology

Boron isotopic composition of tourmaline from massive sulfide deposits and tourmalinites

Martin R. Palmer[1,*] **and John F. Slack**[2]

[1] Department of Earth, Atmospheric and Planetary Sciences, E34-201, Massachusetts Institute of Technology, Cambridge, MA 02139, USA
[2] US Geological Survey, National Center, MS 954, Reston, VA 22092, USA

Abstract. Boron isotope ratios ($^{11}B/^{10}B$) have been measured on 60 tourmaline separates from over 40 massive sulfide deposits and tourmalinites from a variety of geologic and tectonic settings. The coverage of these localities is global (5 continents) and includes the giant ore bodies at Kidd Creek and Sullivan (Canada), Broken Hill (Australia), and Ducktown (USA). Overall, the tourmalines display a wide range in $\delta^{11}B$ values from -22.8 to $+18.3‰$. Possible controls over the boron isotopic composition of the tourmalines include: 1) composition of the boron source, 2) regional metamorphism, 3) water/rock ratios, 4) seawater entrainment, 5) temperature of formation, and 6) secular variations in seawater $\delta^{11}B$. The most significant control appears to be the composition of the boron source, particularly the nature of footwall lithologies; variations in water/rock ratios and seawater entrainment are of secondary importance. The boron isotope values seem especially sensitive to the presence of evaporites (marine and non-marine) and carbonates in source rocks to the massive sulfide deposits and tourmalinites.

Introduction

Massive sulfide deposits are of interest from both a commercial and a scientific point of view. Economically, they constitute a major source of many important metals, especially Cu, Pb, Zn, and Ag. Scientific interest centers on the spatial and secular relationship of massive sulfides to local and global tectonic events, and on the geochemical processes that form the deposits (e.g., Franklin et al. 1981; Gustafson and Williams 1981). Massive sulfide deposits are an expression of large-scale, high-temperature, seawater-lithosphere interactions (including sediments and volcanics) that have a profound influence on the chemistry of the oceans.

Recent studies have shown that tourmaline is an accessory gangue mineral in many massive sulfide deposits (Slack 1982). Tourmaline is a complex borosilicate with the basic formula $NaR_3Al_6B_3Si_6O_{27}(OH,F)_4$, where R is predominantly Fe^{2+} in schorl, Mg in dravite, and (Al+Li) in elbaite. Na may be partially to completely replaced by Ca in uvite if valency conditions are satisfied (Deer et al. 1986). Tourmaline also has other, less common, endmembers and may contain a wide variety of trace elements (e.g., Dietrich 1985). Tourmaline has a rhombohedral unit cell, with the boron occurring as distorted planar BO_3 groups (Deer et al. 1986; Dietrich 1985). In massive sulfide deposits it occurs in four main types of settings (Slack 1982): 1) disseminations in the main sulfide bodies, 2) concentrations in feeder zones and alteration pipes, 3) fillings of metamorphic fractures in wall rocks, and 4) stratabound layers of tourmaline-rich rock or tourmalinite. The nature of tourmaline occurrence may vary among deposits, and it commonly is present in several different forms within an individual sulfide body. Electron microprobe analyses show that massive-sulfide tourmalines fall mainly within the schorl-dravite solid solution series, with a tendency for Mg-rich compositions to predominate (Ethier and Campbell 1977; Taylor and Slack 1984; Plimer 1988; Slack and Coad 1989). These studies, together with trace element and oxygen and hydrogen isotope analyses (Taylor and Slack 1984), indicate that tourmalines from such massive sulfide environments are derived from submarine hydrothermal fluids, and are not inherited from detrital sedimentary or plutonic granitic sources.

Tourmalinites are stratabound rocks containing in excess of 15–20% tourmaline (Nicholson 1980; Slack 1982). Tourmalinites form volumetrically minor, but diagnostically important, lithologies in close association with a variety of stratabound mineral deposits including those containing base metals, gold, tungsten, tin, cobalt, and uranium (Slack et al. 1984). Many tourmalinites are stratiform and bedded, even within complexly deformed terranes, and are believed to have formed by syngenetic or diagenetic processes prior to metamorphism. Some workers have invoked a purely exhalative genesis for tourmalinites (e.g., Plimer 1986; 1988), but definitive evidence for a syngenetic origin is lacking in most cases, and it is likely that many tourmalinites formed by the selective replacement of permeable sediments or volcanics in the upper parts of submarine hydrothermal systems (J.F. Slack, in preparation). The origin of tourmalinites in metaevaporite sequences is more problematic, particularly because of the probable role played by borates in the early history of such sequences, and because of uncertainties surrounding the paragenesis of tourmaline relative to possible boron-rich precursors (Slack et al. 1984). Tourmalines from metaevaporite and carbonate-rich terranes are characteristically dravites or uvites (Schreyer and Abraham 1976; Dunn et al. 1977; Brown and Ayuso 1985),

* *Present address:* Department of Geology, University of Bristol, Queen's Rd., Bristol BS8 1RJ, UK

Offprint requests to: M.R. Palmer

whereas tourmalines from non-evaporitic clastic metasedimentary and metavolcanic terranes typically have compositions intermediate between schorl and dravite (Ethier and Campbell 1977; Appel and Garde 1987; Plimer 1988).

In submarine hydrothermal systems boron is believed to be leached from footwall rocks by convecting hydrothermal fluids (Slack 1982; Plimer 1988). The footwall rocks in such systems can include sediments, volcanics, and evaporites. In clastic sediments and some altered volcanics (e.g., rhyolites), clays (particularly illite) may contain as much as 2000 ppm boron (Harder 1959) which is easily leached during hydrothermal alteration; highly soluble borate minerals constitute another source of readily extractable boron. The boron leached from footwall rocks is transported as complex molecules (e.g., $B(OH)_3$), and under favorable conditions is precipitated in a boron-rich mineral at or below the rock (or sediment)-water interface. In ancient massive sulfide deposits and tourmalinites the precipitated boron mineral probably was tourmaline (Plimer 1988; Slack and Coad 1989), although other precursors are possible. For the purposes of this paper we assume that tourmaline was the initial hydrothermal precipitate, and that no other boron-rich minerals formed during diagenesis or metamorphism.

Boron isotope geochemistry

Boron forms simple oxy- and fluoro-compounds that are volatile and soluble in aqueous phases. Boron is never bound directly to cations and shows no changes in redox state. Boron isotopes (^{11}B and ^{10}B) can be separated by simple ion exchange procedures (Kakihana et al. 1977). In aqueous systems the isotope fractionation is controlled by the distribution of isotopes between the trigonal boric acid molecule $B(OH)_3$ and the coexisting tetrahedral borate anion $B(OH)_4^-$. Theoretical calculations and experiments have shown this fractionation to be about 23‰ at 25° C, with the anion being depleted in ^{11}B (Kotaka 1973; Kakihana et al. 1977). Given the high molecular weight of these reacting species, equilibrium fractionation processes are completely dominant. Boric acid has a pKa of about 8 at room temperature (Culberson and Pytkowicz 1967; Hershey et al. 1986) with the pKa increasing with temperature (Mesmer et al. 1972); hence, the relative abundances of $B(OH)_3$ and $B(OH)_4^-$ are a sensitive function of pH, which lies in the range 4–9 for most natural waters. Because the trigonal species takes part in solid-solution reactions rather than the total boron in solution, and because the boron isotopic composition of each species is dependant on their relative abundance (Palmer et al. 1987), the isotope fractionation factor in water-rock reactions is pH-dependant. Almost all high-temperature, submarine hydrothermal fluids have pH values of <6, where $B(OH)_4^-$ is a negligible portion of the total boron in solution (Spivack et al. 1987; Palmer et al. 1987).

The exact mechanism of tourmaline precipitation from solution is uncertain, but boron uptake in all solid-solution reactions involving aluminosilicates appears to proceed by the same mechanism. The initial step by which boron is incorporated into aluminosilicate structures is the adsorption of $B(OH)_3$ by α-Al_2O_3 surfaces to form a simple surface complex (Bassett 1976); adsorption of polyanionic boron species and $B(OH)_4^-$ is negligible (Bassett 1976; Palmer et al. 1987). Isotopic equilibrium is thus established between the adsorbed and dissolved species, i.e.,

$$^{10}B(OH)_3 + \alpha\text{-}Al_2O_3^- {}^{11}B(OH)_3 \rightleftharpoons {}^{11}B(OH)_3 + \alpha\text{-}Al_2O_3^- {}^{10}B(OH)_3$$

As with aqueous boron the equilibrium lies to the right, because ^{11}B is preferentially partitioned into the trigonal species and ^{10}B is partitioned into the tetrahedral species (in this case α-$Al_2O_3^-B(OH)_3$). The adsorbed boron is then incorporated into the mineral structure without further isotope fractionation. Therefore, in fluid-rock reactions involving precipitation of a boron-bearing mineral, the solid phase (e.g., tourmaline) will be isotopically lighter than the fluid phase (e.g., hydrothermal fluids).

The absolute values for isotope fractionation factors for particular reactions are still largely unknown. Experimental studies of boron isotope fractionation between tourmaline and fluid are currently in progress (M.R. Palmer and D. London, unpublished data), but kinetic problems may make it difficult to carry out experiments below 450° C. The results of this preliminary experimental work suggest that tourmaline-fluid fractionation is approximately 2–3‰ at 750° C and 4–5‰ at 450° C. From the empirical observations of Palmer et al. (1987) it is probable that at room temperature the fractionation is on the order of 20–30‰. Boron isotope data from the Guaymas Basin hydrothermal system (Spivack et al. 1987) suggest that under the submarine hydrothermal conditions of that area (250–300° C), $\delta^{11}B$ fractionation between fluid and boron-bearing hydrothermal precipitates (possibly tourmaline) is approximately 10–14‰.

A variety of fluid and solid boron reservoirs are known in nature which show an extensive range in $\delta^{11}B$ values (Fig. 1). In seawater, boron is a conservative element with a concentration of 420 μmoles/kg (4.6 ppm) and a uniform $\delta^{11}B$ value of +39.5‰. Fresh mid-ocean ridge basalts (MORB) from the East Pacific Rise (EPR) have 0.4 to 0.5 ppm boron and $\delta^{11}B$ values of −3.6 to −2.2‰. The boron content of altered MORB strongly correlates with whole rock $\delta^{18}O$, indicating that boron concentration varies with the degree of alteration. Samples of altered MORB containing 9–69 ppm boron have $\delta^{11}B$ values of +0.1 to +9.2‰; serpentinized peridotites with 50–81 ppm boron have $\delta^{11}B$ values of +8.3 to +12.6‰ (Spivack and Edmond 1987). Continental crust, including island arc volcanics, has $\delta^{11}B$

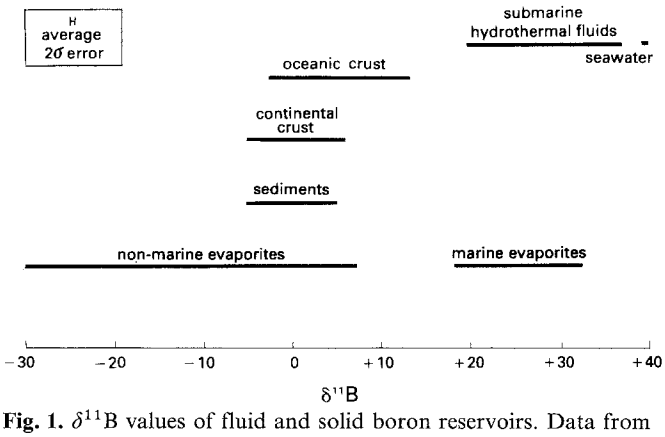

Fig. 1. $\delta^{11}B$ values of fluid and solid boron reservoirs. Data from Spivack (1986), Swihart et al. (1986), and M.R. Palmer (unpub. data)

values from −5.3 to +6.3‰; a similar range (−4.3 to +2.8‰) is observed for terrigenous marine sediments (Spivack 1986; Spivack and Edmond 1987; Spivack et al. 1987). The $\delta^{11}B$ of marine evaporite borates ranges from +18 to +32‰, compared to −30 to +7‰ for borates from non-marine evaporite sequences (Swihart et al. 1986). The greater isotopic range in borate samples from non-marine settings reflects the large variation in $\delta^{11}B$ observed for fresh waters (Spivack 1986).

Large-scale boron exchange occurs between oceanic crust and seawater at high and low temperatures. Hydrothermal solutions venting from mid-ocean ridge crests have boron concentrations that are 10–35% enriched relative to that of seawater, with $\delta^{11}B$ values ranging from +26 to +37‰. Hot spring fluids from the Marianas back-arc spreading center have boron concentrations double that of seawater and a $\delta^{11}B$ value of +20‰. Based on mixing relationships, these results show that in ridge-crest hydrothermal systems boron is quantitatively extracted from basalts with no resolvable isotopic fractionation and added to seawater boron that passes through the system (Spivack and Edmond 1987; Campbell et al. 1988b).

The Guaymas Basin hydrothermal system, Gulf of California, is located within a rift composed of spreading centers and transform faults that comprise a northern extension of the EPR. High sedimentation rates there have buried the spreading axis under as much as 500 m of sediment (Lonsdale and Becker 1985). In the Guaymas hydrothermal system, seawater is drawn down through the sediment and vents onto the seafloor. The chemistry of the hydrothermal fluids rising through the basalt-sediment interface is thought to be similar to those exiting vents on sediment-starved ridge axes. After exiting the oceanic crust, these fluids undergo further reaction with the sediment which substantially alters their chemistry (Von Damm et al. 1985a; Bowers et al. 1985), yielding boron concentrations 3–4 times that of seawater and $\delta^{11}B$ values of +16.5 to +23.2‰ (Spivack et al. 1987). Sediments from DSDP hole 477 in the Guaymas Basin have boron concentrations that range from <1 ppm in hydrothermally altered (greenschist-facies) sections, to 62 ppm in unaltered sections ($\delta^{11}B = -1.2$‰); sediments containing boron in predominantly secondary phases have a $\delta^{11}B$ value of −9.0‰ (Spivack et al. 1987). To date, no hydrothermal tourmaline has been described in the DSDP sediments recovered from Guaymas Basin. Tourmaline may, however, be currently forming in the Guaymas hydrothermal system. Using the thermodynamic data of Kuyunko et al. (1984), Spivack (1986) calculated that the Guaymas vent fluids are saturated with respect to Mg-tourmaline, the most common variety observed in sediment-hosted, stratabound mineral deposits (Taylor and Slack 1984; J.F. Slack, unpublished data).

Previous studies of the boron isotopic composition of tourmaline have used varying methods of extraction and analysis, and have generally provided data for only a few samples of unspecified origin (e.g., Shima 1963; Agyei and McMullen 1968; Malinko et al. 1982). Recently Swihart and Moore (1989) reported boron isotopic analyses of tourmaline from 18 pegmatitic and sedimentary localities, the latter including some inferred submarine-exhalative environments. Our study, begun in 1986, is restricted to analyses of samples containing only one borosilicate (tourmaline), thus eliminating potential complications of inter-mineral fractionation of boron isotopes. We have also limited our investigation to one broad class of rocks and ores (tourmalinites and massive sulfide deposits), which allows general correlations to be made between the boron isotope data and the geologic setting of the samples.

Methods

Boron isotopic analyses were made on tourmaline separates prepared from crushed rocks and sulfide ores. Most analyzed samples were >99% pure, but some contained minor amounts (<10%) of other minerals (chiefly quartz and sulfides). In the absence of other boron-bearing phases (e.g., feldspar, muscovite, sillimanite), total sample purity is not required. The $\delta^{11}B$ values of the tourmalines were determined by thermal ionization mass spectrometry of a cesium metaborate complex following quantitative extraction of the boron by pyrohydrolysis of 1–2 mg of sample (Spivack and Edmond 1986).

The boron isotopic compositions of the samples are reported in the conventional per mil (‰) notation:

$$\delta^{11}B(‰) = \left(\left(\frac{^{11}B/^{10}B \text{ sample}}{^{11}B/^{10}B \text{ standard}}\right) - 1\right) \times 10^3 - 0.19$$

where 0.19 is an oxygen isotope correction factor, and the standard is NBS boric acid SRM 951 (prepared from a Searles Lake borax) which has a $^{11}B/^{10}B$ ratio of 4.04558. The $^{11}B/^{10}B$ ratio of this standard has no intrinsic significance (such as the bulk Earth value), but it does fall approximately in the center of the range of boron isotopic compositions observed in nature (−30 to +40‰).

The in-run precision for a single analysis can be better than ±0.2‰ (2σ), but the reproducibility of isotopically homogeneous samples (e.g., seawater) is approximately ±0.35‰. Replicate analyses of tourmalines made for several samples from this study generally agree within this limit, but some samples show differences that lie outside this precision. In particular, two analyses of a sample from the Ore Knob mine, North Carolina (no. 11119/29), yield $\delta^{11}B$ values of −2.19 and −1.66‰ ($\Delta = 0.53$‰). This sample shows well-developed optical and chemical zoning within individual tourmaline crystals (Slack 1982; Taylor and Slack 1984) and it is possible that boron isotopic zoning may also exist. The bulk sampling technique employed in this study does not allow us to examine this possible effect in detail, but variations in the boron isotopic composition within any one sample are likely to be small (probably on the order of 1 to 3‰) relative to the total range observed in the data set (41‰), hence we do not believe that these variations significantly affect the interpretations presented below.

Results

We have measured the $\delta^{11}B$ values of 60 tourmaline separates from over 40 massive sulfide deposits and tourmalinites. The sample coverage is global (13 countries; 5 continents) and includes specimens from several of the world's largest massive sulfide deposits (i.e., Sullivan, British Columbia; Kidd Creek, Ontario; Ducktown, Tennessee; and Broken Hill, New South Wales), as well as tourmalinites from a variety of metasedimentary and metavolcanic terranes. In Tables 1–3 the samples are grouped by their geologic settings, together with the analytical results and information on location, age, metamorphic grade, and associated mineralization. Brief mineralogic descriptions of the samples and their regional and local settings are given in the Appendices.

The total range of tourmaline $\delta^{11}B$ values measured in this study is −22.8 to +18.3‰. With a typical precision of ±0.35‰ this constitutes a dynamic range of over 100 (total measured range/analytical precision). Our preliminary data indicate that variations in boron isotopic compo-

Table 1. $\delta^{11}B$ values of tourmaline samples from dominantly clastic metasedimentary terranes

Sample no.	$\delta^{11}B$	Associated mineralization	Location	Age	Metamorphic grade	References
EZ-272	-14.17 ± 0.23 (-14.23 ± 0.17)	Cu, Zn, Ag	Elizabeth mine, Vermont	Devonian(?)	Amphibolite	1, 2
JS-80-58A	-13.05 ± 0.35	Cu, Zn, Ag	Elizabeth mine, Vermont	Devonian(?)	Amphibolite	1, 2
PH-810-9	-13.88 ± 0.35 (-13.80 ± 0.34)	Cu, Zn	Pike Hill mine, Vermont	Devonian(?)	Amphibolite	2, 3
CP-16	-15.37 ± 0.28	Cu, Zn	Ely mine, Vermont	Devonian(?)	Amphibolite	2, 3
11119/29	-2.19 ± 0.23 (-1.66 ± 0.61)	Cu, Zn	Ore Knob mine, North Carolina	Late Proterozoic	Amphibolite	4, 5
JS-81-52-6	-5.54 ± 0.36	Mn, Au	Zoar area, Massachusetts	Ordovician	Greenschist	6, 7
JS-81-70	-6.56 ± 0.40	Pb, Zn, Ag	Sullivan mine, British Columbia	Middle Proterozoic	Greenschist	8, 9, 10
Sull-84-1	-2.85 ± 0.30	Pb, Zn, Ag	Sullivan mine, British Columbia	Middle Proterozoic	Greenschist	8, 9, 10
BB-NW-2271	-8.14 ± 0.30	Cu, Co, Au	Blackbird district, Idaho	Middle Proterozoic	Amphibolite	11, 12
R-173-71	-13.71 ± 0.35	Fe, Au	Keystone area, South Dakota	Middle Proterozoic	Amphibolite	13, 14
JS-79-24F	-10.52 ± 0.24	Cu, Zn, Pb, Ag	Black Hawk mine, Maine	Ordovician(?)	Greenschist	15, 16
CUY-526	-5.17 ± 0.34	Fe	Cuyuna Range, Minnesota	Early Proterozoic	Greenschist	17, 18
JS-82A-24F	-13.78 ± 0.31	Au	Golden Dyke dome, N. Territory	Middle Proterozoic	Greenschist	19, 20
BH-18	-13.82 ± 0.32	Pb, Zn, Ag	Broken Hill mine, South Africa	Early Proterozoic	Amphibolite	21, 22
HP-388	-8.14 ± 0.36	Cu, Zn	Gorob prospect, Namibia	Late Proterozoic	Amphibolite	23, 24
JS-87NB-9A	-8.22 ± 0.36	None	Onguati area, Namibia	Late Proterozoic	Greenschist	25, 26
Kilembe-1	-7.74 ± 0.34	Cu	Kilembe mine, Uganda	Early(?) Proterozoic	Amphibolite	27, 28, 29
JS-79N-1	-12.11 ± 0.24 (-12.79 ± 0.26)	Pb, Zn, Ag	Bleikvassli mine, Nordland, Norway	Late Proterozoic	Amphibolite	30, 31
JS-79N-3	-11.94 ± 0.36	Pb, Zn, Ag	Bleikvassli mine, Nordland, Norway	Late Proterozoic	Amphibolite	30, 31
329926	-11.32 ± 0.43	W	Store Malene, West Greenland	Archaean	Amphibolite	32, 33, 34
343610	-10.42 ± 0.36	W	Store Malene, West Greenland	Archaean	Amphibolite	32, 33, 34
78100409	-2.78 ± 0.38	Cu	Sazare mine, Shikoku, Japan	Permian(?)	Greenschist	35, 36, 37
T (K)/2/89	-13.02 ± 0.35	Zn	Kolari mine, Nagpur, India	Early(?) Proterozoic	Greenschist	38, 39, 40

$\delta^{11}B$ values in parentheses are repeat analyses of the sample above

References. *1* Howard (1969); *2* Annis et al. (1983); *3* White and Eric (1944); *4* Kinkel (1967); *5* Taylor and Slack (1984); *6* Chidester et al. (1967); *7* Slack et al. (1983); *8* Freeze (1966); *9* Hamilton et al. (1982); *10* Nesbitt et al. (1984); *11* Anderson (1947); *12* Nash and Hahn (1989); *13* Norton (1976); *14* Raymond (1981); *15* LaPierre (1977); *16* Slack (1980); *17* Schmidt (1963); *18* Morey (1983); *19* Nicholson (1980); *20* Plimer (1986); *21* Ryan et al. (1986); *22* P.G. Spry (personal communication, 1986); *23* Killick (1983); *24* Preussinger (1987); *25* F.P. Badenhorst (personal communication, 1987); *26* F.P. Badenhorst and J.F. Slack (unpublished field data); *27* Tanner (1972); *28* Warden (1985); *29* G.E. Ray (personal communication, 1987); *30* Ramberg (1967); *31* Vokes (1963); *32* Appel (1985); *33* Appel and Garde (1987); *34* Appel (1988); *35* Kanehira and Tatsumi (1970); *36* Takeda (1970); *37* Ito (1984); *38* Bandyopadhyay et al. (1988); *39* Naqvi and Rogers (1987); *40* B.K. Bandyopadhyay (personal communication, 1989)

sition can exist both on a district and deposit scale. For example, in the Broken Hill (Australia) district (Table 3), $\delta^{11}B$ values for 8 samples range from -22.8 to $-17.2‰$. A similar spread is seen for some individual ore bodies, such as Kidd Creek, Ontario (Table 2), where $\delta^{11}B$ values range from -13.6 to $-10.1‰$ (2 samples), and Sullivan, British Columbia (Table 1), where $\delta^{11}B$ values range from -6.6 to $-2.9‰$ (2 samples). As noted above, it is possible that variations of several per mil may also exist for zoned tourmaline crystals within individual samples. Such $\delta^{11}B$ variations show that one analysis does not uniquely characterize an individual massive sulfide body or tourmalinite. However, the limited range in $\delta^{11}B$ values observed for each deposit ($<5‰$) is far less than the difference in $\delta^{11}B$ values between different types of deposits, hence we feel that broad interpretations can be made on the basis of one analysis.

A comparison of the data in Tables 1–3 with the geologic descriptions presented in Appendices I–III reveals no obvious relationship between $\delta^{11}B$ values and the mineralogy of a sample, nor with the size or age of an associated deposit. In addition, available microprobe data suggest that there is no overall correlation between the chemical and boron isotopic composition of the analyzed tourmalines.

Discussion

A number of possible factors may control the boron isotopic composition of tourmalines in massive sulfide deposits and tourmalinites. The principal controls are likely to be: 1) temperature of formation, 2) regional metamorphism, 3) water/rock ratios, 4) seawater entrainment, 5) secular variations in the $\delta^{11}B$ value of ancient seawater, and 6) composition of the boron source. As a guide to the following discussion these processes are schematically illustrated in Fig. 2. The starting fluid is assumed in most cases to be seawater that reacts with a reservoir containing a more or less well-constrained boron concentration and isotopic composition, to produce a hydrothermal fluid with a characteristic boron signature. The final stage represents the boron isotopic composition and relative abundance of tourmaline precipitated from the fluid. At this time it is not possible to produce a more quantitative model because of the preliminary nature of our understanding of boron isotope systematics. Moreover, the boron reservoirs illustrated in step two of Fig. 2 represent endmember cases, and obviously more than one of these reservoirs may have been present in the source rocks to an individual deposit. The effects of seawater entrainment and variable water/rock

Table 2. $\delta^{11}B$ values of tourmaline samples from dominantly metavolcanic terranes

Sample no.	$\delta^{11}B$	Associated mineralization	Location	Age	Metamorphic grade	References
JS-82A-17D	-1.49 ± 0.33	Zn, Pb, Cu, Ag, Au	Rosebery mine, Tasmania	Cambrian	Greenschist	1, 2
JG-64D-77	-2.05 ± 0.35	Fe, Au	Dillwyn area, Virginia	Cambrian(?)	Amphibolite	3, 4
V-1193	-4.72 ± 0.37	Cu, Zn	Armenius mine, Virginia	Cambrian(?)	Amphibolite	4, 5
KC-3005	-13.56 ± 0.34	Cu, Zn, Pb, Ag	Kidd Creek mine, Ontario	Archaean	Greenschist	6, 7, 8
KC-3459	-10.09 ± 0.38	Cu, Zn, Pb, Ag	Kidd Creek mine, Ontario	Archaean	Greenschist	6, 7, 8
Ming-1	-6.11 ± 0.35	Cu, Au	Ming mine, Newfoundland	Ordovician	Greenschist	9, 10
Pecos-1	-15.17 ± 0.39 (-14.88 ± 0.39)	Pb, Zn, Cu, Ag	Pecos mine, New Mexico	Early Proterozoic	Amphibolite	11, 12, 13
JS-81-78	-15.27 ± 0.27	Cu, Zn	Jones mine, New Mexico	Early Proterozoic	Greenschist	12, 13
Rudkins-2	-15.71 ± 0.38	Cu, Zn	Rudkins mine, Bagdad, Arizona	Early Proterozoic	Greenschist	14, 15
VAX-38R	-10.62 ± 0.32	Cu, Zn	Prieska mine, South Africa	Early Proterozoic	Granulite	16, 17
PR-D-353D	-9.39 ± 0.22	Cu, Zn	Prieska mine, South Africa	Early Proterozoic	Granulite	16, 17
JS-82F-15A	-9.75 ± 0.39	Cu, Zn	Pyhasalmi mine, western Finland	Middle Proterozoic	Amphibolite	18, 19
JS-82F-16D	-12.32 ± 0.25	Cu, Zn	Pyhasalmi mine, western Finland	Middle Proterozoic	Amphibolite	18, 19
JS-82F-28G	-1.92 ± 0.38 (-1.52 ± 0.36)	Cu, Zn, Pb	Vihanti mine, western Finland	Middle Proterozoic	Amphibolite	20, 21
JS-82N-1	-1.63 ± 0.36 (-1.95 ± 0.21)	Cu, Zn	Vassfjell area,[a] Trondheim, Norway	Cambrian	Greenschist	22, 23, 24
JS-86S-10	-2.51 ± 0.34	Cu, Zn	Kristineberg mine, Skellefte, Sweden	Middle Proterozoic	Greenschist	25, 26
T(RM)/6/89	-13.24 ± 0.37	Cu	Ran Mangli mine, Nagpur, India	Early(?) Proterozoic	Greenschist	27, 28, 29

$\delta^{11}B$ values in parentheses are repeat analyses of the sample above

[a] from the Flalokken mine (Carstens 1942)

References. *1* Green et al. (1981); *2* Plimer and Lees (1988); *3* Brown (1969); *4* Pavlides et al. (1982); *5* Cox (1979); *6* Walker et al. (1975); *7* Beaty et al. (1988); *8* Slack and Coad (1989); *9* Tuach and Kennedy (1978); *10* Tuach (1984); *11* Krieger (1932); *12* Riesmeyer (1978); *13* Robertson and Moench (1979); *14* Anderson et al. (1955); *15* Conway (1986); *16* Wagener and van Schalkwyk (1986); *17* Theart et al. (1989); *18* Huhtala (1979); *19* Helovuori (1979); *20* Rouhunkoski (1968); *21* Rauhamaki et al. (1978); *22* Carstens (1942); *23* Grenne et al. (1980); *24* Taylor and Slack (1984); *25* Rickard and Zweifel (1975); *26* Willden (1986); *27* Bandyopadhyay et al. (1988); *28* Naqvi and Rogers (1987); *29* B.K. Bandyopadhyay (personal communication, 1989)

Table 3. $\delta^{11}B$ values of tourmaline samples from metaevaporite and carbonate-associated terranes

Sample no.	$\delta^{11}B$	Associated mineralization	Location	Age	Metamorphic grade	References
NM-GO-1	-4.15 ± 0.34	None	Farm Gurumanas, Namibia	Late Proterozoic	Greenschist	1, 2
NM-GO-2	-8.13 ± 0.39	None	Farm Gurumanas, Namibia	Late Proterozoic	Greenschist	1, 2
NM-Stolz-1	$+18.32\pm0.32$	None	Farm Stolzenfeld, Namibia	Late Proterozoic	Greenschist	3, 4, 5
JS-87NB-10A	-3.63 ± 0.34	None	Ondundu area, Namibia	Late Proterozoic	Greenschist	6, 7
EB-67-90	$+10.47\pm0.36$ ($+10.63\pm0.45$)	None	Gouverneur area, New York	Late Proterozoic	Amphibolite	8, 9
JS-87-1	$+6.65\pm0.37$	None	Arnold talc mine, New York	Late Proterozoic	Amphibolite	10, 11, 12
PQ-Pap-D8	-4.18 ± 0.42	None	Papaskwasati Fm, central Quebec	Early Proterozoic	Greenschist	13, 14
PQ-Pap-D9	-7.35 ± 0.40	None	Papaskwasati Fm, central Quebec	Early Proterozoic	Greenschist	13, 14
MM-81-10-04	$+1.56\pm0.36$	Zn, Pb, Au, Ag	Montauban mine, southern Quebec	Late Proterozoic	Amphibolite	15, 16
HU-113776	$+2.29\pm0.39$	Zn, Mn	Sterling Hill mine, New Jersey	Late Proterozoic	Granulite	17, 18
CK-1073/46	$+3.22\pm0.40$	Cu, Zn	Cherokee mine, Ducktown, Tennessee	Late Proterozoic	Amphibolite	19, 20, 21
BH-961-1067	-22.48 ± 0.32	Pb, Zn, Ag	Globe mine, BHD	Middle Proterozoic	Granulite	22, 23, 24
JS-82A-1A	-18.98 ± 0.38 (-18.97 ± 0.38)	Pb, Zn, Ag	Copper King mine, BHD	Middle Proterozoic	Granulite	22, 23, 24
JS-82A-2-1	-19.71 ± 0.24	Co	Stirling Vale area, BHD	Middle Proterozoic	Granulite	22, 23, 24
JS-82A-3	-20.83 ± 0.37	None	Pinnacles area, BHD	Middle Proterozoic	Granulite	22, 23, 24
JS-82A-11F	-17.92 ± 0.40	Pb, Zn, Ag	Black Prince mine, BHD	Middle Proterozoic	Amphibolite	22, 23, 24, 25
JS-82A-13B	-17.23 ± 0.35	Pb, Zn, Ag	Jersey Lily mine, BHD	Middle Proterozoic	Amphibolite	22, 23, 24, 25
JS-82A-14B	-22.79 ± 0.23	W	Yanco Glen area, BHD	Middle Proterozoic	Amphibolite	22, 23, 24, 25, 26
JS-82A-16C	-21.88 ± 0.38	W	Corruga prospects, BHD	Middle Proterozoic	Granulite	22, 23, 24, 26
Ficht-1	-12.29 ± 0.35	None	Fichtelgebirge area, West Germany	Cambrian(?)	Greenschist	27, 28

$\delta^{11}B$ values in parentheses are repeat analyses of the sample above

BHD Broken Hill District, New South Wales (Australia)

References. *1* Behr et al. (1983); *2* H. Porada and J.F. Slack (unpublished field data); *3* Uhlig (1987); *4* Schalk (1988); *5* Porada and Behr (1988); *6* Preussinger (1987); *7* F.P. Badenhorst (personal communication, 1987); *8* Bannerman (1972); *9* Brown and Ayuso (1985); *10* Lea and Dill (1968); *11* deLorraine and Dill (1982); *12* Ayuso and Brown (1984); *13* Caty (1976); *14* Chown (1987); *15* Stamatelopoulou-Seymour and MacLean (1984); *16* Bernier et al. (1987); *17* Palache (1935); *18* Hague et al. (1956); *18* Emmons and Laney (1926); *20* Nesbitt (1979); *21* Slater (1982); *22* Willis et al. (1983); *23* Plimer (1983); *24* Haydon and McConachy (1987); *25* Barnes (1980); *26* Barnes (1983); *27* Mielke and Schreyer (1969); *28* Abraham et al. (1972)

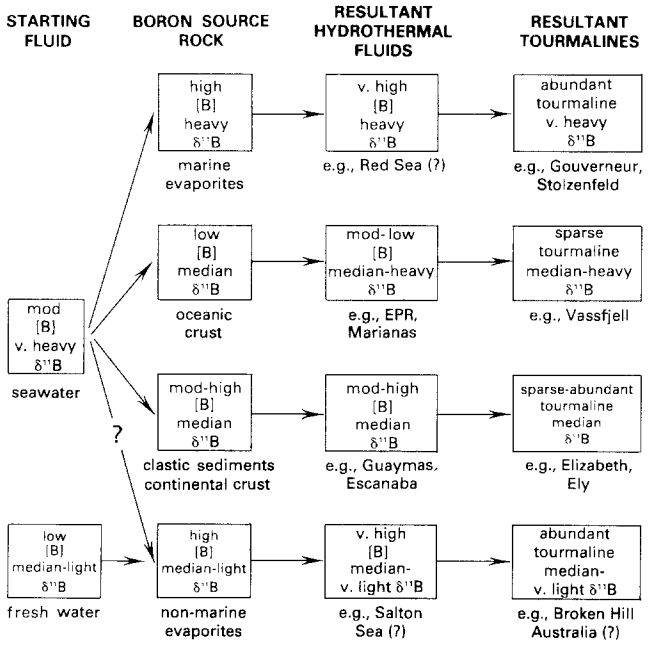

Fig. 2. Schematic diagram of boron isotope systematics of hydrothermal fluids and tourmalines. Adjectives describing the various properties are relative. [*B*] represents the concentration of boron in the hydrothermal fluid

ratios, in addition, cause subtle changes in $\delta^{11}B$ values of the tourmalines. Metamorphism may also play a role in determining the measured $\delta^{11}B$ values. In the following sections we examine each of these processes to assess their relative importance for producing the range in $\delta^{11}B$ values observed for all of the samples, and for selected individual deposits.

Temperature of formation

The temperatures of the fluids from which the tourmalines formed have undoubtedly varied among samples. Changes in temperature may affect the boron isotopic fractionation between tourmaline and fluid, so that lower temperature processes would be expected to produce greater isotopic fractionation than would higher temperature processes. We cannot as yet quantitatively evaluate such temperature effects, but some empirical evidence exists from $\delta^{11}B$ data for tourmalines from different types of massive sulfide deposits. Tourmalines from dominantly cupriferous massive sulfides, such as those sampled from the U.S. Appalachians, for example, presumably formed at higher temperatures than did tourmalines from Pb–Zn deposits elsewhere. Samples from the cupriferous Appalachian ore bodies have $\delta^{11}B$ values that range from −15.4‰ for Ely, Vermont (CP-16) to +3.2‰ for Ducktown, Tennessee (CK-1073/46). Tourmalines from Pb–Zn massive sulfides display a similar wide range of $\delta^{11}B$ values from −22.5‰ for a sample from the Globe mine in the Broken Hill district, Australia (BH-961-1067) to +1.6‰ for a tourmalinite from the Montauban mine, Quebec (MM-81-10-04). The lack of any systematic difference between the boron isotopic composition of tourmalines from these two diverse groups of massive sulfide deposits suggests that variations in the temperature of formation of the tourmalines was not a dominant process controlling the observed range in $\delta^{11}B$ values. A similar conclusion has been reached by Musashi et al. (1988) with respect to regional boron isotope variations in hot spring waters of Japan. Experimental studies of tourmaline-fluid fractionation of boron isotopes, currently in progress (M.R. Palmer and D. London, unpublished data), should provide a more definitive answer to this question.

Regional metamorphism

The massive sulfide deposits and tourmalinites from which the samples were taken have all undergone regional metamorphism that ranges from lower greenschist to granulite facies (Tables 1–3). In this context we use the term metamorphism to refer to changes in mineral assemblages and textures that accompany deep burial and tectonism, and that postdate initial crystallization of tourmaline. We draw a distinction between this regional metamorphism and submarine hydrothermal metamorphism (e.g., Evarts and Schiffman 1983). The effects of regional metamorphism on the $\delta^{11}B$ values cannot as yet be rigorously evaluated, but there is some evidence to suggest that tourmalines may be fairly resistant to isotopic fractionation during metamorphism.

Tourmaline, which typically contains about 10 wt% B_2O_3, is the only significant reservoir of boron within the sulfide deposits and tourmalinites. Other possible boron-bearing phases in the analyzed samples are garnet, feldspar, muscovite, and sillimanite. In certain unusual environments these minerals may contain up to 1 wt% B_2O_3 (Grew and Hinthorne 1983; Smith and Brown 1988), but they typically have boron contents of <0.1 wt% B_2O_3 (Harder 1974; Erd 1980; Jones and Smith 1984; Shaw et al. 1988). Boron loss from high-grade regional metamorphic terranes has recently been reported (Truscott and Percival 1988; Sisson et al. 1988), but the presence of tourmaline concentrations in some granulite-facies sequences (e.g., Broken Hill, Australia: Barnes 1980; Plimer 1983) indicates that boron loss during metamorphism is not universal. Experimental studies by Robbins and Yoder (1962) showed that dravite is stable up to temperatures of about 865° C and water pressures of 1–2 kb; Manning (1981) determined that quartz-schorl assemblages do not melt below 850° C at 1 kb. Although tourmaline commonly recrystallizes during metamorphism, it clearly has a wide stability range (e.g., Werding and Schreyer 1984). When tourmaline breaks down the boron released can follow one of a number of different paths depending on the metamorphic conditions. If boron is not expelled from the system it will be reincorporated into recrystallized metamorphic tourmaline or into kornerupine, grandidierite, or sapphirine, depending on various $P-T-X$ conditions (Manning and Pichavant 1983; Grew 1988). None of our samples contain kornerupine (or other borosilicates), thus potential fractionation of boron isotopes between tourmaline and other minerals is not a factor in this study.

The histogram in Fig. 3 is patterned according to the metamorphic grade of the terranes containing the analyzed samples. Overall, there appears to be a slight tendency for samples from the most strongly metamorphosed sequences to have the isotopically lightest boron, but there is considerable overlap among the $\delta^{11}B$ values of tourmalines from different metamorphic grades. It is noteworthy that data for granulite-facies terranes span much of the total range of our measured boron isotopic compositions for tourmaline, including those from Broken Hill, Australia (−22.8 to −19.0‰); Prieska, South Africa (−10.6 and −9.4‰);

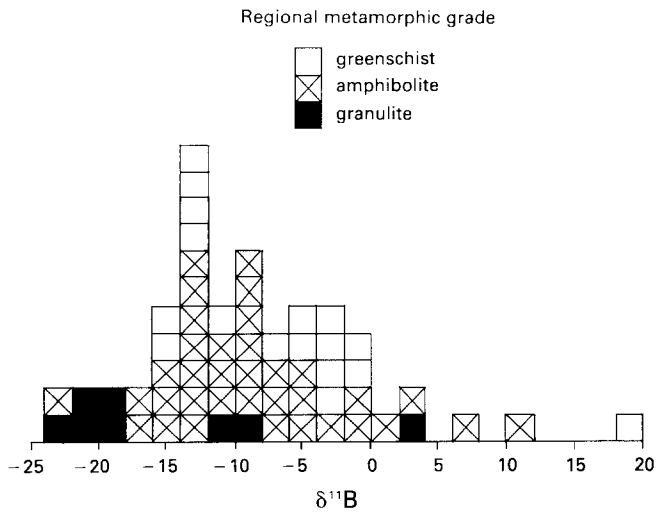

Fig. 3. Histogram of $\delta^{11}B$ values of tourmalines versus regional metamorphic grade of the associated massive sulfide deposits and tourmalinites

and Sterling Hill, New Jersey (+2.3‰). Swihart and Moore (1989) also report a $\delta^{11}B$ value of +22‰ for tourmaline from a kornerupine-bearing granulite-facies sequence at Lac Ste.-Marie, Quebec.

The critical factor controlling the behavior of boron isotopes in tourmalines during metamorphism is likely to be the activity of a fluid phase. When fluid activity is low or metamorphism isochemical, the $\delta^{11}B$ values of tourmalines will, in theory, be unaffected. If there is loss of boron from the system any recrystallized tourmalines/would most likely have isotopically lighter boron compared to original (premetamorphic) tourmalines, because ^{11}B is preferentially partitioned into fluid phases. Low-temperature boron loss during diagenesis and greenschist-facies metamorphism, however, could produce even greater isotopic fractionation than that under amphibolite- and granulite-facies conditions. This possibility cannot be completely dismissed, but on balance we concur with Swihart and Moore (1989) that the diagenetic and metamorphic history of the samples is not the dominant control determining the $\delta^{11}B$ values of tourmalines from metasedimentary and metavolcanic terranes.

Water/rock ratios

The concept of water/rock (W/R) ratios has been widely used in studies of water-rock interactions involving oxygen and hydrogen isotopes (e.g., Taylor 1974), but the term has also been successfully applied to elements such as boron and the alkalis that are readily leached from rocks by circulating fluids (Von Damm et al. 1985b; Spivack and Edmond 1987; Campbell et al. 1988b). For example, W/R ratios calculated for hydrothermal systems from the EPR on the basis of boron isotope systematics give identical results to those obtained from oxygen isotope studies (Spivack and Edmond 1987).

Submarine hydrothermal fluids that have reacted only with basalt have high $\delta^{11}B$ values (+20 to +37‰) because unaltered basalts have low boron concentrations (<1 ppm) and, hence, comparatively little isotopically light boron is added to the original high $\delta^{11}B$ of seawater (+39.5‰). Clastic sediments have much higher boron concentrations (up to hundreds of ppm) so that submarine hydrothermal fluids that have also reacted with sediments overlying oceanic crust have higher boron concentrations, and, prior to secondary mineral (e.g., tourmaline) precipitation, much lower $\delta^{11}B$ values (Spivack and Edmond 1987; Spivack et al. 1987; Campbell et al. 1988b). Thus, where all other conditions are equal (lithologic setting, temperature, etc.) and where marine evaporites are not contained in the sequence, tourmalines precipitated from high W/R ratio fluids (i.e., those that have not experienced significant clastic-sediment interaction) would be expected to have higher $\delta^{11}B$ values than those precipitated from low W/R fluids (i.e. those that have experienced a greater degree of reaction with sediments).

Evidence of W/R controls on tourmaline $\delta^{11}B$ values comes from data for dominantly sediment-hosted, cupriferous massive sulfides of the U.S. Appalachians (see Kinkel 1967; Gair and Slack 1980). We have measured the $\delta^{11}B$ values of tourmaline samples from five of these deposits (Ore Knob, North Carolina; Ducktown, Tennessee; Black Hawk, Maine; Ely and Elizabeth, Vermont). Metamorphism has typically reached middle amphibolite facies in the area of the deposits, but textural evidence suggests that the associated tourmalines, although variably recrystallized, originally formed by syngenetic and/or diagenetic processes concurrently with the massive sulfides (Slack 1982; Taylor and Slack 1984). The sulfide ore bodies are enclosed by clastic metasedimentary rocks interpreted as metamorphosed marine turbidites, with only minor proportions of intercalated tholeiitic metabasalt (amphibolite). No stratigraphically related evaporites or primary carbonate units are apparent in the footwall or surrounding rocks to any of the deposits[1], except Ducktown which has large lenses of calcite marble locally within the ore ("limestone" of Emmons and Laney 1926). The sulfide mineralogy is relatively constant in nearly all the ore bodies, consisting of massive pyrrhotite, minor chalcopyrite and sphalerite, generally sparse pyrite and arsenopyrite, and only rare galena; Black Hawk contains significant sphalerite and galena locally. Based on available evidence, these deposits can be construed to consist of a largely sediment-hosted ore body underlain (at generally indeterminate depth) by a mafic volcanic substrate related to the heat source that powered hydrothermal circulation.

A plot of $\delta^{11}B$ versus $\delta^{18}O$ for the Appalachian tourmaline samples shows a clear, non-linear, inverse relationship (Fig. 4). The large range in $\delta^{18}O$ for these samples (+8.0 to +15.5‰) has been interpreted to reflect differences in the W/R ratios and footwall lithologies of the deposits, with the highest $\delta^{18}O$ values (i.e., at Ely) being indicative of a greater sedimentary component (Taylor and Slack 1984). The concave nature of the curve in Fig. 4 supports such a mechanism, as comparatively little reaction with sediments is required to change the $\delta^{11}B$ of hydrothermal solutions, whereas the $\delta^{18}O$ systematics are considerably more buffered and require extensive sediment interaction to produce a major isotopic change in the fluid.

Some of the features of the Ore Knob deposit (which

[1] The stratigraphic footwall to the Vermont deposits (White and Eric 1944; Annis et al. 1983) consists at depth (>300 m) of the Waits River Formation which contains abundant carbonate in micaceous schists and minor marbles. These lithologies are interpreted as deep-water turbidites, however, and not shallow-water platform carbonates (Hatch 1988)

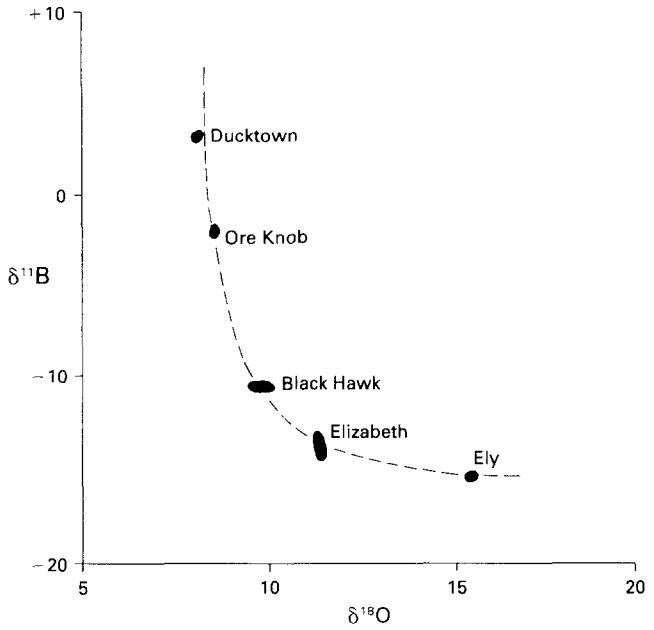

Fig. 4. $\delta^{11}B$ versus $\delta^{18}O$ for tourmalines from cupriferous Appalachian massive sulfide deposits. $\delta^{18}O$ data from Taylor and Slack (1984, Table 8) and B.E. Taylor (personal communciation, 1988)

has nearly the highest $\delta^{11}B$ and lowest $\delta^{18}O$ values in tourmalines) were interpreted by Kinkel (1967) to represent mineralization in a pre-existing fault zone which has subsequently undergone further movement. Such features are proposed in the Guaymas Basin and appear to act as conduits for convecting hydrothermal fluids, reducing their interaction with sediments and consequently resulting in fluids that contain a stronger seawater component (Gieskes et al. 1982; Lonsdale and Becker 1985; Campbell et al. 1988a).

For a given hydrothermal system there are limits to the range of $\delta^{11}B$ values that can result from changes in W/R ratios. The high concentrations of boron characteristic of clastic sediments mean that the $\delta^{11}B$ values of the hydrothermal fluids are dominated by that of the sediments even with relatively little sediment involvement. This is seen in Fig. 4 where $\delta^{11}B$ values of the tourmalines reach a minimum, even though the $\delta^{18}O$ values are still rising, due to continuing reaction with the sediments. An upper limit to the $\delta^{11}B$ values of the tourmalines is established by the fact that the hydrothermal fluids must undergo sufficient reaction with sediments to raise their boron concentrations above a saturation level required for tourmaline precipitation (or some boron-rich precursor). High-quality thermodynamic data are not available to quantify this limit, but in the absence of carbonate and evaporite sediments in the footwall sequences to these Appalachian deposits (excepting Ducktown), the tourmalines appear to reach an upper $\delta^{11}B$ value of approximately 0‰ based on W/R considerations.

Seawater entrainment

Submarine hydrothermal fluids commonly show evidence for entrainment of ambient seawater into the upper portion of convection cells prior to venting onto the seafloor (Bowers et al. 1985). Seawater contains boron that is isotopically heavier than that of hydrothermal fluids which have reacted with basalt or sediment (Fig. 1). The boron isotopic composition of tourmaline precipitated within the upper portions of a massive sulfide body could, therefore, be very sensitive to entrainment of small amounts of seawater. We have analyzed two samples from the Sullivan (British Columbia) Pb−Zn−Ag deposit that may record this process. A sample of cherty tourmalinite from the tourmaline-rich footwall zone (JS-81-70) has a $\delta^{11}B$ value of −6.6‰, compared to a distinctly heavier value of −2.8‰ for a sample of euhedral tourmaline crystals (Sull-84-1) from within the massive pyrrhotite body located near the top of the stratigraphic section (see Hamilton et al. 1982, Fig. 6). This variation in $\delta^{11}B$ values is consistent with entrainment of isotopically heavy seawater during formation of the latter sample. A similar pattern is observed for the Elizabeth Cu−Zn deposit (Vermont), where tourmaline from the massive chalcopyrite-pyrrhotite ore has a $\delta^{11}B$ value of −14.2‰, while tourmaline from a stratigraphically overlying tourmalinite (Annis et al. 1983) has a $\delta^{11}B$ value of −13.1‰. For both deposits, the variations in boron isotopic composition that can be ascribed to seawater entrainment (<5‰) are small relative to the total range observed for all of the analyzed samples (41‰).

Secular variations in seawater $\delta^{11}B$

Previous workers have documented variations in the sulfur and oxygen isotope composition of ancient seawater (Sangster 1968; Claypool et al. 1980), and it is possible that there have also been secular variations in the $\delta^{11}B$ value of seawater. As noted above, however, there is no apparent correlation between the age of the massive sulfide deposits and tourmalinites and the $\delta^{11}B$ values of the analyzed tourmalines. This suggests that if the boron isotopic composition of seawater varied throughout geologic time, it did not exert a significant control over the $\delta^{11}B$ values of tourmalines within massive sulfide deposits and tourmalinites. This interpretation is in accord with the previous discussion of W/R ratios, i.e., that the concentration of boron in sediments is so much greater than that in seawater that the former dominates the boron isotopic composition of hydrothermal fluids produced during high-temperature, seawater-sediment reactions (Spivack et al. 1987).

Composition of the boron source

Possible sources of boron within the tourmalines include basement crustal rocks, terrigenous marine sediments, marine evaporites and carbonates, non-marine evaporites and carbonates, island arc volcanics, altered oceanic crust, and seawater. The $\delta^{11}B$ values of these sources (Fig. 1) show a total range of nearly 70‰. In addition to having distinct boron isotopic compositions, the different reservoirs also have varying boron concentrations. Both factors are of importance in determining the $\delta^{11}B$ values and relative abundance of tourmaline precipitating from submarine hydrothermal fluids (Fig. 2). The geologic settings of the analyzed massive sulfide deposits and tourmalinites are shown in Fig. 5, with an emphasis on the nature of the footwall lithologies.

Massive sulfide deposits near Vassfjell, Norway (Grenne 1980; Grenne et al. 1980) and at Rambler-Ming, Newfoundland (Tuach and Kennedy 1978; Hibbard 1983) are in ophiolite settings[2] dominated by metabasalt. The $\delta^{11}B$ values of tourmalines from these two deposits (Table 2) are −1.6 (−1.9) and −6.1‰, respectively, which are

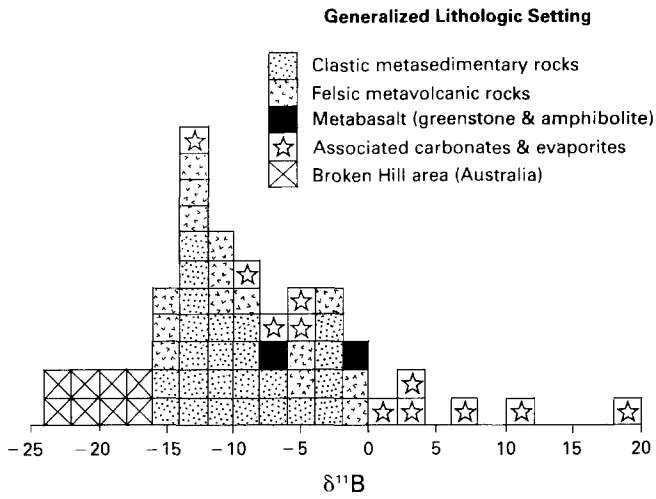

Fig. 5. Histogram of $\delta^{11}B$ values of tourmalines versus dominant footwall lithologies of the associated massive sulfide deposits and tourmalinites

greater than most of those from predominantly sediment-hosted massive sulfides and tourmalinites. Fluids from active hydrothermal systems on sediment-starved ridge crests have lower boron concentrations and higher $\delta^{11}B$ values than those from sediment-covered ridges because basalt contains low boron concentrations, and, hence, contributes less isotopically light boron to the hydrothermal fluid than does sediment (Spivack and Edmond 1987; Spivack et al. 1987). Tourmalines precipitated from fluids in sediment-starved hydrothermal systems should, therefore, have greater $\delta^{11}B$ values than those from sediment-dominated systems; this is supported by our data for the Ming and Vassfjell samples. The presence of minor rhyolite in the footwall to the Ming ore body (Tuach 1984) probably contributes to the isotopically lighter boron in the Ming tourmaline relative to that from Vassfjell.

Samples from settings dominated by clastic metasediments (Table 1) form a group with $\delta^{11}B$ values ranging from -15.4 to $-1.7‰$. Prominent massive sulfide deposits within this group include Elizabeth, Vermont (-14.2 and $-13.0‰$); Ore Knob, North Carolina ($-1.9‰$); Black Hawk, Maine ($-10.5‰$); Sullivan, British Columbia (-6.6 and $-2.8‰$); Bleikvassli, Norway (-12.5 and $-11.9‰$); Kilembe, Uganda ($-7.7‰$); Broken Hill, South Africa ($-13.8‰$); and Sazare, Japan ($-2.8‰$). These data and those for sediment-hosted tourmalinites are centered around a $\delta^{11}B$ value of approximately $-10‰$. This is similar to the value of $-9‰$ measured in altered sediments from the Guaymas Basin hydrothermal system that appear to contain secondary boron derived from the hydrothermal fluids (Spivack et al. 1987). In contrast, $\delta^{11}B$ values of unaltered sediments from Guaymas Basin ($-1.2‰$) fall roughly in the middle of the range measured for clastic marine sediments (-4.3 to $+2.8‰$) and continental/arc crust (-5.3 to $+6.3‰$), so that the clustering of the tourmaline data around the $\delta^{11}B$ value of altered sediments at Guaymas lends support to this type of model for the formation of most sediment-hosted deposits considered here.

[2] The paleotectonic setting of the Ming and related massive sulfide deposits is controversial and both ophiolitic (e.g, Hibbard 1983) and primitive island arc (e.g., Hutchinson 1973) settings have been proposed. The area is, however, principally underlain by tholeiitic and bonninitic metabasalts (Gale 1973; Swinden et al. 1989)

Massive sulfide deposits from island arc and other rhyolitic volcanic terranes (Table 2) have tourmalines with $\delta^{11}B$ values of -15.7 to $-1.5‰$. Important deposits within this group include Rosebery, Tasmania ($-1.5‰$); Kidd Creek, Ontario (-13.6 and $-10.1‰$); Pecos, New Mexico ($-15.0‰$); Prieska, South Africa (-10.9 and $-9.4‰$); Pyhasalmi, Finland (-12.3 and $-9.8‰$); Vihanti, Finland ($-1.7‰$); and Kristenberg, Sweden ($-2.5‰$). The range of $\delta^{11}B$ values shown by this group of samples is nearly identical to that of the sediment-hosted deposits (Table 1) and reflects the similar boron isotopic compositions (Spivack 1986) of island arc volcanics (-5 to $+6‰$) and terrigenous marine sediments (-4 to $+3‰$). The range of $\delta^{11}B$ values observed for the two groups is believed to mainly reflect variations in temperature, W/R ratio, and/or $\delta^{11}B$ of the source. More detailed work will be needed to discriminate among these variables.

Several samples have $\delta^{11}B$ values that are higher than would appear compatible with a clastic sediment or crustal boron source. It is likely that the actual range of $\delta^{11}B$ values in terrigenous marine sediments and crustal rocks extends beyond that measured to date (Spivack 1986; Spivack et al. 1987), but extreme values would have to be postulated for sedimentary and crustal boron isotope reservoirs to account for the highest $\delta^{11}B$ values observed in the tourmalines. Of major significance is the fact that *all* of the massive sulfide deposits and tourmalinites with $\delta^{11}B$ values $>0‰$ have stratigraphically associated marine evaporite or carbonate beds (Fig. 5). Elsewhere, such reservoirs contain high concentrations of isotopically heavy boron (Swihart et al. 1986). Based on the arguments presented above and the geologic settings of the analyzed samples (see Appendices), we believe that marine evaporites and carbonates are major sources of isotopically heavy boron for the tourmalines with $\delta^{11}B > 0‰$, and may be important components in others as well. Although the $\delta^{11}B$ values of borates from nonmarine evaporites extend up to $+7‰$, it should be remembered that $\delta^{11}B$ values of the tourmalines must be lower than the fluid from which they precipitated, and thus lower than their solid boron reservoirs. Therefore, if nonmarine evaporites were a major source of boron to the hydrothermal fluids then any resultant tourmalines should have $\delta^{11}B$ values significantly less than $+7‰$.

Tourmaline samples from the northwest Adirondacks of New York, including the Gouverneur area (EB-67-90) and the Arnold talc mine (JS-87-1) in the Balmat-Edwards zinc district, have $\delta^{11}B$ values of $+10.5$ and $+6.7‰$[3], respectively. These samples are from terranes that contain evidence of metaevaporites stratigraphically associated with the tourmaline-bearing units including talc-tremolite schists and chlorine-bearing scapolite granulites in the Gouverneur area (Brown and Ayuso 1985), and massive bedded anhydrite in the Balmat mine sequence (Lea and Dill 1968; de Lorraine and Dill 1982). The Balmat sequence also locally contains well-preserved domal stromatolites (Isachsen and Landing 1983) indicative of shallow-water deposition. The

[3] Swihart and Moore (1989) report a $\delta^{11}B$ value of $+12‰$ for manganoan uvite-dravite from the Balmat area. Their sample (USNM #133996) is from the No. 1 talc mine near Talcville (M. Mopper, personal communication, 1989); it is not the material analyzed by Ayuso and Brown (1984) which is catalogued as USNM #116009/14. Our sample (JS-87-1) and that of Swihart and Moore (1989) are both from unit 13 in the Balmat sequence (cf. de Lorraine and Dill 1982, Fig. 2)

Late Proterozoic Grenville Complex, from which these samples were taken, has undergone multiple periods of deformation and regional metamorphism to upper amphibolite (sillimanite) facies. Despite this deformation and high grade of metamorphism, tourmalines from these terranes have preserved what appear to be primary high $\delta^{11}B$ values characteristic of a marine evaporite source for the contained boron. Non-marine evaporite sources are precluded in both cases.

We have analyzed several tourmalinites from the Late Proterozoic Damara orogen of central Namibia. Three samples are from the Duruchaus Formation that is believed to have developed in a non-marine evaporite setting during the initial rifting stages of the orogen (Porada and Wittig 1983; Miller 1983b; Porada and Behr 1988). Within this group of samples, NM Stolz-1 from the Farm Stolzenfeld shows a clear association with thin dolomite beds (Uhlig 1987), contains relict evaporite crystal cavities (J.F. Slack, unpublished field data, 1987), and has a high boron isotope signature of $+18.3‰$, compared to values of -4.2 and $-8.1‰$ in samples NM-GO-1 and NM-GO-2 from the Farm Gurumanas Oos located within the same sedimentary formation. The relatively low $\delta^{11}B$ values for the Gurumanas tourmalinites are compatible with a non-marine evaporite origin for the boron in the tourmalines, but the very high $\delta^{11}B$ value for the Stolzenfeld tourmalinite is clearly inconsistent with this model (see Fig. 1), and may reflect diagenetic formation of tourmaline during incursion of a marine sabkha facies interpreted by Behr et al. (1983) to post-date deposition of the Duruchaus Formation[4].

Three samples have also been analyzed from the younger Kuiseb Formation in Namibia that formed during the later stages of continental rifting associated with the generation of an incipient oceanic spreading center (Miller 1983a). This spreading center consisted of a sediment-covered ridge crest comprised of clastic marine turbidites (the Kuiseb Formation), tholeiitic basalt (the Matchless amphibolite), and locally associated serpentinites, massive sulfide deposits, and tourmalinites. Samples from the surface gossan of the small Gorob sulfide body (HP-388) and a tourmalinite located within the Kuiseb Formation distal from the massive sulfides (JS-87NB-10A) have similar $\delta^{11}B$ values (-8.1 and $-8.2‰$, respectively). In contrast is sample JS-87NB-9A from the base of the Kuiseb Formation at Ondundu, where tourmalinite units are directly underlain by the Karibib Formation which contains thick carbonate beds (Porada and Wittig, 1983) with local evaporite relicts (F.P. Badenhorst, oral communication, 1987); the quartzose sequence hosting the tourmalinites there also has evaporite crystals and crystal cavities (J.F. Slack, F.P. Badenhorst, and P. Charles, unpublished field data, 1987). The $\delta^{11}B$ value of this sample ($-3.6‰$), which is significantly greater than that of the tourmalinites stratigraphically higher in the Kuiseb Formation, is interpreted as having been increased by a component of isotopically heavy boron derived from marine evaporites in the underlying Karibib Formation.

Although obvious evaporite features are retained in some weakly metamorphosed sequences (e.g., Stolzenfeld), it is likely that other tourmaline-bearing deposits containing evaporitic boron may be in settings that have not preserved evaporites. In addition to the metamorphic and tectonic events that might remove evidence of any original boron-bearing source rocks, evaporites typically are readily destroyed by low-intensity chemical and physical processes (e.g., diagenesis, erosion). Unusual chemical compositions of metamorphic rocks and minerals have been used to infer the prior existence of evaporites in high-grade metasedimentary sequences (e.g., Schreyer and Abraham 1976; Moine et al. 1981), but these studies have not distinguished between marine and non-marine evaporites (Hardie 1984). The presence of heavy boron isotopic compositions in tourmalines may therefore provide evidence for the involvement of marine evaporites in a terrane that might not otherwise be apparent. It is interesting to note that a sample from the carbonate-hosted Sterling Hill zinc deposits in New Jersey (HU-113776) has a $\delta^{11}B$ value of $+2.3‰$. This value is distinctly higher than that for other tourmalines from predominantly sediment- or rhyolite-hosted deposits. Recent oxygen isotope data suggest that the present ore and gangue minerals in this Zn–Mn ore body are the result of essentially isochemical metamorphism of deposits originally formed in a Red Sea-type environment, and were not formed from infiltrating metamorphic fluids from country-rock granites (Johnson et al. 1987). The boron isotope data are compatible with this interpretation.

A tourmaline sample from Ducktown, Tennessee, also has a relatively high $\delta^{11}B$ value of $+3.2‰$. Emmons and Laney (1926) noted the presence of large limestone lenses within some of the massive sulfide deposits in this district, and at the same stratigraphic level distal to the ore bodies. The isotopically heavy boron at Ducktown may be derived from this carbonate source, and also could have a component of marine evaporitic borate. This possibility is supported by the recent recognition by J.E. Gair of the US Geological Survey (personal communication, 1988) of anomalous lithium (up to 440 ppm) in several samples of micaceous wall rocks to the Ducktown ore bodies.

The tourmalinite sample from the Montauban Zn–Pb–Au–Ag deposit in southern Quebec (MM-81-10-04) has a somewhat high $\delta^{11}B$ value of $+1.6‰$. The local setting of this deposit consists of clastic metasediments and minor metabasalts, but without associated evaporite beds. The tourmalinite is believed to be coeval with, but distal to, the main orebody which is located within a calc-silicate/carbonate layer that has been considered the metamorphic product of an impure limestone (Stametelopoulou-Seymour and MacLean 1984; Bernier et al. 1987). This stratigraphic interpretation is consistent with the boron isotope data which suggest that the tourmalinite was derived from fluids that passed through and leached boron from marine limestone originally associated with the Montauban ore-forming sequence.

The large Vihanti and Pyhasalmi massive sulfide deposits in western Finland are the same age and occur in broadly similar settings, yet tourmalines from the two deposits have very different $\delta^{11}B$ values (-1.7 and $-11.0‰$, respectively). Post-ore metamorphism has been intense in both areas (upper amphibolite facies), but apparently equivalent in style and degree (Huhtala 1979; Helovuori 1979), so it appears that the variation in tourmaline $\delta^{11}B$ values from the two ore bodies is a primary feature. The major lithologic difference between the deposits is that the footwall to the

[4] Behr et al. (1983) described the occurrence of tourmalinites in the Duruchaus Formation. Since that work, recent field study has cast doubt on the stratiform nature of all the Gurumanas tourmalinites (Porada and Behr 1988). The tourmalinite on the Farm Stolzenfeld does appear stratiform, however (Uhlig 1987)

Vihanti ores contains dolomite and phosphorite beds of marine origin (Rehtijarvi et al. 1979). Primary boron in these (or related) dolomites would, therefore, be expected to have high $\delta^{11}B$ values. Leaching of boron in (or associated with) these beds by hydrothermal fluids represents a likely source of the isotopically heavy boron identified at Vihanti.

Evaporites may also have contributed components to the Rosebery polymetallic massive sulfide deposit in western Tasmania. This rich Zn–Pb–Cu–Ag–Au orebody, one of several massive sulfides within the Cambrian Mt. Read Volcanics, is hosted in a thin siltstone unit underlain by massive rhyolite pyroclastics (Green et al. 1981). Concentrations of tourmaline are present in several parts of the orebody (Plimer and Lees 1988), some of which may have formed during emplacement of post-ore Devonian granites (Solomon et al. 1987). We have not analyzed delicately zoned euhedral tourmalines which fill open space in magnetite-rich parts of the orebody that are probably the result of Devonian remobilization. We have, however, analyzed a tourmalinite that forms a concordant stratabound unit in the hangingwall of F lens. A Devonian origin for this tourmalinite cannot be entirely excluded, but it contains foliated tourmaline and pyrite grains that suggest formation prior to deformation and granite intrusion (J.F. Slack, unpublished data). The $\delta^{11}B$ value of $-1.5‰$ determined for this hangingwall tourmalinite sample (JS-82A-17D) is higher than those of most other sediment- and/or rhyolite-hosted deposits, and suggests a component of marine evaporite boron in the tourmaline. The recent identification of evaporites in western Tasmania in Proterozoic basement units beneath the Mt. Read Volcanics (Anderson, in Plimer and Lees 1988) supports this hypothesis. Such a model would require deep circulation by the submarine hydrothermal system that formed the Rosebery deposit.

Tourmalines from the Broken Hill (Australia) district (Table 3) have the isotopically lightest boron measured for any of our samples and are outlined separately in Fig. 5. A detailed boron isotopic investigation of this region is currently in progress so only a brief discussion of our initial data (Slack et al. 1987) will be presented here. This district contains the giant Broken Hill Pb–Zn–Ag orebody, which is one of the world's largest and most thoroughly studied massive sulfide deposits. Despite this its origin remains the subject of considerable debate. Part of the problem in determining the genesis of the ores is that the mid-Proterozoic Willyama Supergroup, which hosts the deposit, has undergone extensive deformation and metamorphism that have obscured most primary depositional features (e.g., Stevens 1986). The present metamorphic lithologies have been interpreted as representing a variety of paleoenvironments, including evaporitic fluvio-lacustrine, saline alkaline, deep marine, intracratonic, and volcano-sedimentary. A deep-water, volcano-sedimentary exhalative origin has been the most widely accepted (e.g., Stanton 1972; Plimer 1985), but a marine/non-marine prograding deltaic complex has recently been suggested as the original host lithology (Haydon and McConachy 1987), with the ore bodies having been formed in coarse sands during compactive expulsion of deep-seated brines (Wright et al. 1987). In considering how the boron isotope data address this problem we must first examine the effects of high grade metamorphism at Broken Hill.

The metamorphic grade of the district ranges from amphibolite facies in the northwest to granulite facies in the southeast (Phillips 1980; Stevens 1986). High-grade metamorphism does not per se lead to the alteration of $\delta^{11}B$ values in tourmaline unless significant amounts of boron are removed (or introduced) during metamorphic event(s). The isotopically lightest value measured to date from Broken Hill ($-22.8‰$) is for a tourmalinite from near Yanco Glen (JS-82A-14B), which is in the area of lowest (andalusite-muscovite) metamorphic grade, and throughout the district there is no systematic correlation between $\delta^{11}B$ values of the tourmalines and metamorphic grade of the host rocks. For example, fine-grained tourmalines from tourmalinite layers that show clear evidence of primary sedimentary features (graded bedding, flame structures, etc.: Barnes 1980; Slack et al. 1984) are isotopically indistinguishable from coarse-grained tourmalines that have undergone extensive recrystallization. We cannot, as yet, dismiss metamorphic fractionation as a cause of the low $\delta^{11}B$ values there, but we do not find any of the expected correlations with metamorphic features and boron isotope ratios that would support this hypothesis. From the measured range in pelagic sediment/crustal $\delta^{11}B$ values (Fig. 1) it is apparent that changes in W/R ratios could not have produced the large quantities of low $\delta^{11}B$ tourmaline at Broken Hill. Again, it may be argued that the original crust and/or sediments at Broken Hill had very low $\delta^{11}B$ values or that the tourmalines originally formed at low (i.e., $<200°$ C) temperatures, but we suggest an alternative explanation. In keeping with recently proposed models for the district involving shallow water sedimentation (N. Herriman, personal communication to JFS, 1984; Wright et al. 1987; Stevens et al. 1988), we suggest that the isotopically light boron at Broken Hill may have been derived from non-marine evaporites, as this is the only known reservoir containing sufficiently light boron to explain the tourmaline $\delta^{11}B$ values. Our detailed boron isotope study of the Broken Hill block (in progress) with B.P.J. Stevens will allow a more rigorous evaluation of this model.

Conclusions

We have analyzed the boron isotopic composition of 60 tourmaline samples from over 40 massive sulfide deposits and tourmalinites from diverse metasedimentary and metavolcanic settings. The worldwide distribution of these localities includes the giant ore bodies at Kidd Creek and Sullivan (Canada), Broken Hill (Australia), and Ducktown (U.S.A.). Overall, the tourmalines display a wide range in $\delta^{11}B$ values from -22.8 to $+18.3‰$. This range reflects the relative contributions of boron (and presumably other elements) from reservoirs that may include marine evaporites and carbonates ($\delta^{11}B = +18$ to $+32‰$), non-marine evaporites and carbonates ($\delta^{11}B = -30$ to $+7‰$), terrigenous marine sediments ($\delta^{11}B = -4$ to $+3‰$), fresh oceanic crust ($\delta^{11}B = -3‰$), altered oceanic crust ($\delta^{11}B = 0$ to $+13‰$), island arc volcanics ($\delta^{11}B = -5$ to $+6‰$), and seawater ($\delta^{11}B = +40‰$). The tourmaline $\delta^{11}B$ values lack any correlation with age, size, mineralogy, or metamorphic grade of the massive sulfide deposits and tourmalinites. The data do, however, show a general correlation with lithologic setting, particularly for samples from inferred marine and some non-marine metaevaporite sequences. The stability of tourmaline and its locus as the only significant reservoir of boron in submarine hydrothermal environments seems to allow it

to preserve premetamorphic $\delta^{11}B$ values, apparently even in granulite-facies terranes. An inverse relationship between $\delta^{11}B$ and $\delta^{18}O$ values in tourmalines from several Appalachian massive sulfides also suggests that the boron isotope data reflect varying water/rock ratios during formation of the deposits.

Boron isotopic analyses of tourmaline may also be used to discriminate between marine and non-marine evaporite sequences. Because of potential isotopic fractionation associated with fluid-solid precipitation and diagenesis or metamorphism, tourmaline $\delta^{11}B$ values represent minimum compositions for the source reservoir(s). Tourmaline $\delta^{11}B$ values $>0‰$ suggest a component of marine evaporite boron, possibly derived from original borate minerals. Identifying non-marine evaporites from tourmaline $\delta^{11}B$ values is problematic because of the greater number of light boron isotope reservoirs in nature (see Fig. 1), and because low-temperature precipitation, diagenesis, and metamorphism can also produce tourmalines with low $\delta^{11}B$ values. Even tourmalinites from well-documented non-marine evaporite sequences, such as those from the Archean Mistassini Group of Quebec (Chown 1987), contain tourmalines with $\delta^{11}B = -4.2$ and $-7.4‰$ (Table 3); these results are similar to those acquired for tourmalines from clastic metasedimentary and rhyolitic metavolcanic terranes (Fig. 5). Despite these uncertainties, boron isotopic analyses of tourmaline could potentially be useful in evaluating whether a metaevaporite sequence has a marine or non-marine heritage.

Acknowledgements. The results of this study were made possible in part by the generous donation of samples by many individuals and institutions. We wish to thank the following for supplying specimens for analysis: P.W.U. Appel, B.K. Bandyopadhyay, H. Banks and the Smithsonian Institution, L. Bernier, C.E. Brown, E.H. Chown, P.R. Coad, C.M. Conway, H.O. Durgin, C.A. Francis and Harvard University, J.E. Gair, T. Grenne, G.A. Hahn, R.L. Hauser, T. Ito, R.S. Mitchell and the University of Virginia, B.E. Nesbitt, H. Porada, H. Preussinger, G.E. Ray, W.H. Raymond, J. Reino, J.M. Robertson, R.G. Schmidt, P.G. Spry, F. Totten, F.M. Vokes, and W. Zobel. Access to drill core and underground mining properties was provided to J.F.S. by Anglo Vaal Corporation, Black Mountain Mineral Development Company Ltd., Boliden Mineral AB, Cominco Ltd. (Canada), Conoco Minerals, Kidd Creek Mines Ltd., Noranda Exploration Inc., North Broken Hill Ltd., Outokumpu Oy, West Coast Mines (Tasmania), and Tennessee Chemical Company. Field assistance and logistical support were also supplied to J.F.S. by F.P. Badenhorst and the Geological Survey of South West Africa/Namibia, R.G. Barnes and the Geological Survey of New South Wales, and by P.M. Nicholson and Gepeko Ltd. Mineral separation work was performed at the US Geological Survey by D.M. Demichelis, K. Fluek-Holveg, S.J. Hilbish, and J.T. Thole. We thank Stan Hart for generous provision of mass spectrometer facilities at M.I.T. and B.E. Taylor (Geological Survey of Canada) for supplying the $\delta^{18}O$ analysis of the Ducktown tourmaline. John M. Edmond provided lab space and a stimulating environment at M.I.T. P.B. Barton, Jr. (US Geological Survey) reviewed an early version of this manuscript and offered many valuable suggestions for its improvement, as did W. Schreyer and two anonymous reviewers. M.R.P. acknowledges the support of a NATO post-doctoral fellowship and NSF grant EAR-8800495 to M.R. Palmer and J.M. Edmond.

Appendix I

Geologic settings of tourmaline samples from dominantly clastic metasedimentary terranes

Sample No.	Sample type	Regional setting	Adjacent wall rocks
EZ-272	Massive Sulfide	Clastic metasediments + minor metabasalts	Actinolite-phlogopite schist; hornblende schist
JS-80-58A	Tourmalinite	Clastic metasediments + minor metabasalts	Actinolite-phlogopite schist; hornblende schist
PH-810-9	Disseminated Tourmaline	Clastic metasediments + minor metabasalts	Calcareous mica schist; amphibolite
CP-16	Disseminated Tourmaline	Clastic metasediments + minor metabasalts	Quartz-mica schist (metapelite); massive sulfide
11119/29	Massive Sulfide	Clastic metasediments + minor metabasalts	Quartz-feldspar granofels (metagreywacke)
JS-81-52-6	Tourmalinite	Metabasalt + metarhyolite + volcaniclastics	Chloritic metasediments + coticule (Mn-garnet) rock
JS-81-70	Tourmalinite	Clastic metasediments + gabbro intrusion	Quartzite + silty argillite, massive Pb-Zn-Ag sulfide
Sull-84-1	Massive Sulfide	Clastic metasediments + gabbro intrusion	Massive sulfide (pyrrhotite)
BB-NW-2271	Tourmalinite	Clastic metasediments + minor metabasalt	Quartzite + minor silty argillite
R-173-71	Tourmalinite	Clastic metasediments + minor metabasalt	Grunerite iron formation
JS-79-24F	Tourmalinite	Clastic metasediments + minor metavolcanics	Metavolcanics + metasediments + post-ore granite pluton
CUY-526	Tourmalinite	Clastic metasediments + minor metabasalts	Bedded iron formation
JS-82A-24F	Tourmalinite	Clastic metasediments + chert + dolerite sills	Mainly siltstone + minor tuffaceous chert
BH-18	Disseminated Tourmaline	Clastic metasediments + minor metabasalt	Amphibolite; magnetite-quartz iron formation; massive sulfide
HP-388	Tourmalinite	Clastic metasediments + minor metabasalt	Massive sulfide; pelitic schist
JS-87NB-9A	Tourmalinite	Clastic metasediments	Quartzite; pelitic schist
Kilembe-1	Massive Sulfide	Clastic metasediments + minor metabasalt	Quartzite; amphibolite + chlorite-biotite schist
JS-79-N1	Disseminated Tourmaline	Clastic metasediments + minor metabasalt	Quartzite; pelitic schist; minor graphitic schist
JS-79-N3	Massive Sulfide	Clastic metasediments + minor metabasalt	Massive sulfide; pelitic schist

Appendix I (continued)
Geologic settings of tourmaline samples from dominantly clastic metasedimentary terranes

Sample No.	Sample type	Regional setting	Adjacent wall rocks
329926	Tourmalinite	Clastic metasediments + metabasalt	Banded amphibolite; pelitic schist; cordierite gneiss
343610	Tourmalinite	Clastic metasediments + metabasalt	Banded amphibolite, pelitic schist, cordierite gneiss
78100409	Massive Sulfide	Clastic metasediments + minor metabasalt	Metabasalt + pelitic schist + quartzite
T (K)/2/89	Tourmalinite	Clastic metasediments + minor metabasalt	Metapelite; mafic flows + tuffs; massive Zn-rich sulfide

Appendix II
Geologic settings of tourmaline samples from dominantly metavolcanic terranes

Sample No.	Sample type	Regional setting	Adjacent wall rocks
JS-82A-17D	Tourmalinite	Metavolcanics + minor clastic metasediments	Metavolcanics
JG-64D-77	Tourmalinite	Metarhyolite + metabasalt	Quartz-magnetite iron formation
V-1193	Disseminated Tourmaline	Metarhyolite + metabasalt	Massive sulfide
KC-3005	Disseminated Tourmaline	Metarhyolite + metabasalt	Mainly brecciated metarhyolite; massive and stringer sulfide
KC-3459	Disseminated Tourmaline	Metarhyolite + metabasalt	Mainly brecciated metarhyolite; massive and stringer sulfide
Ming-1	Massive Sulfide	Metabasalt + minor metarhyolite	Predominantly mafic metavolcanics; massive sulfide
Pecos-1	Tourmalinite	Metavolcanics + minor metasediments	Massive sulfide, metarhyolite
JS-81-78	Disseminated Tourmaline	Metavolcanics + minor metasediment	Chlorite-rich metavolcanics; massive sulfide
Rudkins-2	Tourmalinite	Metarhyolite + minor metabasalts	Massive sulfide; metarhyolite
VAX-38R	Massive Sulfide	Clastic metasediments + metavolcanics	Amphibole-bearing gneiss
PR-D-353D	Tourmalinite	Clastic metasediments + metavolcanics	Amphibole-bearing gneiss; massive sulfide
JS-82F-15A	Massive Sulfide	Metabasalt + metarhyolite + volcaniclastics	Massive sulfide
JS-82F-16D	Massive Sulfide	Metabasalt + metarhyolite + volcaniclastics	Corderite mica gneiss + sericite schist; massive sulfide
JS-82F-28G	Disseminated Tourmaline	Metabasalt + metarhyolite + volcaniclastics	Calc-silicate skarn + dolomite marble; massive sulfide
JS-82-N-1	Massive Sulfide	Metabasalt + metagabbro intrusions	Principally metabasalt
JS-86S-10	Tourmalinite	Clastic metasediments + volcaniclastics	Cherty stratiform quartzite
T (RM)/6/89	Tourmalinite	Rhyolite + rhyodacite metavolcanics	Chloritized felsic volcanics; massive Cu sulfide

Appendix III
Geologic settings of tourmaline samples from metaevaporite and carbonate-associated terranes

Sample No.	Sample type	Regional setting	Adjacent wall rocks
NM-GO-1	Tourmalinite	Non-marine evaporite sequence	Quartzite, pelitic schist
NM-GO-2	Tourmalinite	Non-marine evaporite sequence	Quartzite, pelitic schist
NM-Stolz-1	Tourmalinite	Non-marine evaporite sequence	Quartzite, pelitic schist + dolomite
JS-87NB-10A	Tourmalinite	Clastic metasediments overlying marbles + metaevaporite	Quartzite, pelitic schist
EB-67-90	Tourmalinite	Carbonate + clastic metasediments	Diopside-scapolite paragneiss + quartzofeldspathic granulite
JS-87-1	Disseminated Tourmaline	Carbonate + clastic metasediments	Talc-tremolite schist
PQ-Pap-D8	Tourmalinite	Fluvial arkosic sandstone + quartz-pebble conglomerate	Sandstone, conglomerate
PQ-Pap-D9	Tourmalinite	Fluvial arkosic sandstone + quartz-pebble conglomerate	Sandstone, conglomerate
MM-81-10-84	Tourmalinite	Clastic metasediments + minor metabasalts	Quartzofeldspathic gneiss

Appendix III (continued)
Geologic settings of tourmaline samples from metaevaporite and carbonate-associated terranes

Sample No.	Sample type	Regional setting	Adjacent wall rocks
CK-1073/46	Disseminated Tourmaline	Clastic metasediments + minor amphibolite	Pelitic schist; massive sulfide
HU-113776	Disseminated Tourmaline	Calcite marble	Zn-Mn-Fe oxide ore body
BH-961-1067	Disseminated Tourmaline	Clastic metasediments + minor metavolcanics	Quartzite + metapelite; massive sulfide
JS-82A-1A	Disseminated Tourmaline	Clastic metasediments + minor metavolcanics	Fe-oxide gossan; sillimanite-rich gneiss
JS-82A-2-1	Tourmalinite	Clastic metasediments + minor metavolcanics	Albite-rich granulite
JS-82A-3	Disseminated Tourmaline	Clastic metasediments + minor metavolcanics	Quartzofeldspathic gneiss
JS-82A-11F	Tourmalinite	Clastic metasediments + minor metavolcanics	Pelitic schist; amphibolite
JS-82A-13B	Disseminated Tourmaline	Clastic metasediments + minor metavolcanics	Pelitic schist; quartzite
JS-82A-14B	Tourmalinite	Clastic metasediments + minor metavolcanics	Metapelite + amphibolite + minor pegmatite
JS-82A-16C	Tourmalinite	Clastic metasediments + minor metavolcanics	Pelitic schist; quartzite; amphibolite
Ficht-1	Tourmalinite	Marble + clastic metasediments + minor metabasalts	Quartzite; pelitic schist; carbonate-rich metasediments

References

Abraham K, Mielke H, Povondra P (1972) On the enrichment of tourmaline in metamorphic sediments of the Arzberg Series, W.-Germany (NE-Bavaria). Neues Jahrb Mineral Monatsh 5:209–219

Agyei EK, McMullen CC (1968) A study of the isotopic abundance of boron from various sources. Can J Earth Sci 5:921–927

Anderson AL (1947) Cobalt mineralization in the Blackbird district, Lemhi County, Idaho. Econ Geol 42:22–46

Anderson CA, Scholz EA, Strobell JD Jr (1955) Geology and ore deposits of the Bagdad area, Yavapai County, Arizona. US Geol Surv Prof Paper 278, 103 pp

Annis MP, Slack JF, Rolph AL (1983) Stratabound massive sulphide deposits of the Elizabeth mine, Orange County, Vermont. In: Sangster DF (ed) Field trip guidebook to stratabound sulphide deposits, Bathurst area, N.B., Canada and west-central New England, U.S.A. Geol Survey Canada Misc Rept 36, pp 41–51

Appel PWU (1985) Strata-bound tourmaline in the Archaean Malene supracrustals, West Greenland. Can J Earth Sci 22:1485–1491

Appel PWU (1988) Stratiform tourmalinites in the Archaean tungsten province of West Greenland. Mineral Petrol 39:79–91

Appel PWU, Garde AA (1987) Stratabound scheelite and stratiform tourmalinites in the Archaean Malene supracrustal rocks, southern West Greenland. Gronlands Geol Undersog Bull 156, 26 pp

Ayuso RA, Brown CE (1984) Manganese-rich red tourmaline from the Fowler talc belt, New York. Can Mineral 22:327–331

Bandyopadhyay BK, Roy A, Shukla RS, Sarkar TKG (1988) Bimodal volcanism, massive sulphides and associated Mn garnet-chert rocks in the Proterozoic Sakoli Basin in central India: Examples of metamorphosed mixed volcanic and exhalative-sedimentary type Cu and Zn deposits in a zone of crustal extension. In: Sarkar SC (ed) International Conference on Metallogeny Related to Tectonics of Proterozoic Mobile Belts, IGCP Project 247. Geol Survey India and Jadavpur Univ, Calcutta, Abstracts, pp 27–28

Bannerman HM (1972) Geologic map of the Richville-Bigelow area, St. Lawrence County, New York. US Geol Surv Misc Inv Map I-664, scale 1:18000

Barnes RG (1980) A metallogenic study of the Purnamoota-Yalcowinna 1:50000 sheet, northern Broken Hill block. Geol Surv New South Wales Rept GS 1980/116, 198 pp

Barnes RG (1983) Stratiform and stratabound tungsten mineralisation in the Broken Hill block, N.S.W. J Geol Soc Aust 30:225–239

Bassett RL (1976) The geochemistry of boron in thermal waters. Unpub PhD Thesis, Stanford Univer 236 pp

Beaty DW, Taylor HP Jr, Coad PR (1988) An oxygen isotope study of the Kidd Creek, Ontario, volcanogenic massive sulfide deposit: Evidence for a high ^{18}O ore fluid. Econ Geol 83:1–17

Behr H-J, Ahrendt H, Martin H, Porada H, Rohrs J, Weber K (1983) Sedimentology and mineralogy of Upper Proterozoic playa-lake deposits in the Damara orogen. In: Martin H, Eder FW (eds) Intracontinental fold belts. Springer-Verlag, Berlin Heidelberg New York, pp 577–610

Bernier L, Pouliot G, MacLean WH (1987) Geology and metamorphism of the Montauban north gold zone: A metamorphosed polymetallic exhalative deposit, Grenville Province, Quebec. Econ Geol 82:2076–2090

Bowers TS, Von Damm KL, Edmond JM (1985) Chemical evolution of mid-ocean ridge hot springs. Geochim Cosmochim Acta 49:2239–2252

Brown CE, Ayuso RA (1985) Significance of tourmaline-rich rocks in the Grenville Complex of St. Lawrence County, New York. US Geol Surv Bull 1626C, 33 pp

Brown WR (1969) Geology of the Dillwyn quadrangle, Virginia. Virginia Div Miner Resources, Rept Inv 10, 77 pp

Campbell AC, Bowers TS, Measures CI, Falkner KK, Khadem M, Edmond JM (1988a) A time series of vent fluid compositions from 21° N, East Pacific Rise (1979, 1981, 1985), and the Guaymas Basin, Gulf of California (1982, 1985). J Geophys Res 93:4537–4549

Campbell AC, Palmer MR, Klinkhammer GP, Bowers TS, Edmond JM, Lawrence JR, Casey JF, Thompson G, Humphris S, Rona P, Karson JA (1988b) Chemistry of hot springs on the Mid-Atlantic Ridge: TAG and MARK Sites. Nature 335:514–519

Carstens CW (1942) Turmalin and Fluszspat als Bestandteile von Schwefelkieserz. Kongel Norske Vid Selsk Forh 15:13–16

Caty JL (1976) Région du lac Mistassini, Québec, stratgraphie et sédimentologie de la formation Papaskwasati. Ministère des Richesses Naturelles du Québec, DPV 423

Chidester AH, Hatch NL Jr, Osberg PH, Norton SA, Hartshorn

JH (1967) Geologic map of the Rowe quadrangle, Franklin and Berkshire Counties, Massachusetts, and Bennington and Windham Counties, Vermont. US Geol Surv Map GQ-642, scale 1:24000
Chown EH (1987) Tourmalinites in the Aphebian Mistassini Group, Quebec. Can J Earth Sci 24:826–830
Claypool GE, Holser WT, Kaplan IR, Sakai H, Zak I (1980) The age curves of sulfur and oxygen isotopes in marine sulfate and their mutual interpretation. Chem Geol 28:199–260
Conway CM (1986) Field guide to Early Proterozoic strata that host massive sulfide deposits at Bagdad, Arizona. In: Nations JD, Conway CM, Swann GA (eds) Geology of central and northern Arizona. Geol Soc America, Rocky Mtn Sec Guidebook, pp 104–157
Cox LJ (1979) Mineralogy and petrogenesis of the Armenius deposit, Louisa County, Virginia. Unpub MS Thesis, Virginia Polytech Inst & State Univ, 114 pp
Culberson C, Pytkowicz RM (1967) Effect of pressure on carbonic acid, boric acid and the pH of seawater. Science 157:59–61
Deer WA, Howie RA, Zussman J (1986) Rock-forming minerals 1B (Disilicates and ring silicates). Longman, Essex, UK, 2nd ed., 629 pp
deLorraine WF, Dill DB (1982) Structure, stratigraphic controls, and genesis of the Balmat zinc deposits, northwest Adirondacks, New York. In: Hutchinson RW, Spence CD, Franklin JM (eds) Precambrian sulphide deposits. Geol Assoc Can Spec Paper 25:571–596
Dietrich RV (1985) The tourmaline group. Van Nostrand Reinhold Co., New York, 300 pp
Dunn PJ, Appleman D, Nelen JE, Norberg J (1977) Uvite, a new (old) common member of the tourmaline group and its implications for collectors. Mineral Rec 8:100–108
Emmons WH, Laney FB (1926) Geology and ore deposits of the Ducktown mining district, Tennessee. US Geol Surv Prof Paper 139, 114 pp
Erd RC (1980) Boron in metamorphic rocks. In: Supplement to Mellor's Comprehensive Treatise on Inorganic and Theoretical Chemistry. V (Boron). Longman Group Ltd., London, pp 96–105
Ethier VG, Campbell FA (1977) Tourmaline concentrations in Proterozoic sediments of the southern Cordillera of Canada and their economic significance. Can J Earth Sci 14:2348–2363
Evarts RC, Schiffman P (1983) Submarine hydrothermal metamorphism of the Del Puerto ophiolite, California. Am J Sci 283:289–340
Franklin JM, Lydon JW, Sangster DF (1981) Volcanic-associated massive sulfide deposits. In: Skinner BJ (ed) Econ Geol (75th Anniv Vol), pp 485–627
Freeze AC (1966) On the origin of the Sullivan orebody, Kimberley, B.C. In: Tectonic history and mineral deposits of the western Cordillera. Can Inst Min Metall 8:263–294
Gair JE, Slack JF (1980) Stratabound massive sulfide deposits of the U.S. Appalachians. In: Vokes FM, Zachrisson E (eds) Review of Caledonian-Appalachian stratabound sulphides. Geol Surv Ireland Spec Paper 5:67–81
Gale GH (1973) Paleozoic basaltic komatiite and ocean floor type basalts from northwestern Newfoundland. Earth Planet Sci Lett 18:22–28
Gieskes JM, Kastner M, Einsele G, Kelts K, Niemitz J (1982) Hydrothermal activity in the Guaymas Basin, Gulf of California: A synthesis. In: Initial Rep Deep Sea Drilling Project 64(2):1159–1167
Green GR, Solomon M, Walshe JL (1981) The formation of the volcanic-hosted massive sulfide deposit at Rosebery, Tasmania. Econ Geol 76:304–338
Grenne T (1980) Vassfjell area. In: Wolff FC (ed) Excursions across part of the Trondheim region, central Norwegian Caledonides. Norges Geol Undersok 356:159–164
Grenne T, Grammeltvedt G, Vokes FM (1980) Cyprus-type sulphide deposits in the western Trondheim district, central Norwegian Caledonides. In: Panayiotou A (ed) Ophiolites: Proceedings of the International Ophiolite Symposium, Geol Surv Dept, Nicosia, pp 727–743
Grew ES (1988) Kornerupine at the Sar-e-Sang, Afghanistan, whiteschist locality: Implications for tourmaline-kornerupine distribution in metamorphic rocks. Am Mineral 73:345–357
Grew ES, Hinthorne JR (1983) Boron in sillimanite. Science 221:547–549
Gustafson LB, Williams N (1981) Sediment-hosted stratiform deposits of copper, lead, and zinc. In: Skinner BJ (ed) Econ Geol (75th Anniv Vol), pp 139–178
Hague JM, Baum JL, Herrman LA, Pickering RJ (1956) Geology and structure of the Franklin-Sterling Hill area, N.J. Geol Soc Am Bull 67:435–473
Hamilton JM, Bishop DT, Morris HC, Owens RE (1982) Geology of the Sullivan orebody, Kimberley, B.C., Canada. In: Hutchinson RW, Spence CD, Franklin JM (eds) Precambrian Sulphide Deposits. Geol Assoc Can Spec Paper 25:597–665
Harder H (1959) Beitrag zur Geochemie des Bors. III Bor in Sedimenten. Nach Acad Wissen Gottingen II, Math-Phys Klasse 6:123–175
Harder H (1974) Boron. In: Wedepohl K (ed) Handbook of geochemistry. Springer-Verlag Berlin Heidelberg New York, II, 5-B-1-5-O-10
Hardie LA (1984) Evaporites: Marine or non-marine? Am J Sci 284:193–240
Hatch NL Jr (1988) Some revisions to the stratigraphy and structure of the Connecticut Valley trough, eastern Vermont. Am J Sci 288:1041–1059
Haydon RC, McConachy GW (1987) The stratigraphic setting of Pb–Zn–Ag mineralization at Broken Hill. Econ Geol 82:826–856
Helovuori O (1979) Geology of the Pyhasalmi ore deposit, Finland. Econ Geol 74:1084–1101
Hershey JP, Fernandez M, Milne PJ, Millero FJ (1986) The ionization of boric acid in NaCl, Na–Ca–Cl, Na–Mg–Cl solutions at 25° C. Geochim Cosmochim Acta 50:143–148
Hibbard J (1983) Geology of the Baie Verte Peninsula, Newfoundland. Nfld Dept Mines Energy, Min Devel Div Mem 2, 279 pp
Howard PF (1969) The geology of the Elizabeth mine, Vermont. Vermont Geol Surv, Econ Geol 5, 73 pp
Huhtala T (1979) The geology and zinc-copper deposits of the Pyhasalmi-Pielavesi district, Finland. Econ Geol 74:1069–1083
Hutchinson RW (1973) Volcanogenic sulfide deposits and their metallogenic significance. Econ Geol 68:1223–1247
Isachsen YW, Landing E (1983) First Proterozoic stromatolites from the Adirondack massif: Stratigraphic, structural, and depositional implications. Geol Soc Am Abs Pgms 15:601
Ito T (1984) The chemical composition of tourmaline from the Sazare mine, Ehmine Prefecture and its economic geological significance. J Hokkaido Univ Ed 35(1):63–72 (in Japanese)
Johnson CA, Rye DM, Skinner BJ (1987) Oxygen isotopic compositions of Zn and Mn phases from the Sterling Hill deposit and their genetic implications. Geol Soc Am Abs Pgms 19:718
Jones AP, Smith JV (1984) Ion probe analysis of H, Li, B, F, and Ba in micas, with additional data for metamorphic amphibole, scapolite and pyroxene. Neues Jahrb Mineral Monatsh 5:228–240
Kakihana H, Kotaka M, Shohei S, Nomura M, Okamoto N (1977) Fundamental studies on the ion-exchange separation of boron isotopes. Bull Chem Soc Japan 50:158–163
Kanehira K, Tatsumi T (1970) Bedded cupriferous iron sulphide deposits in Japan, a review. In: Tatsumi T (ed) Volcanism and ore genesis. Univ Tokyo Press, pp 51–76
Killick AM (1983) Sulphide mineralization at Gorob and its genetic relationship to the Matchless member, Damara sequence, SWA/Namibia. In: Miller RMcG (ed) Evolution of the Damara orogen of South West Africa/Namibia. Geol Soc S Afr Spec Publ 11:381–384
Kinkel AR Jr (1967) The Ore Knob copper deposit, North Caro-

lina, and other massive sulfide deposits of the Appalachians. US Geol Surv Prof Paper 558, 58 pp
Kotaka M (1973) Chromatographic separation of boron and nitrogen isotopes using pure water as eluant. Unpub PhD Thesis, Tokyo Inst Technology, 163 pp
Krieger P (1932) Geology of the zinc-lead deposit at Pecos, New Mexico. Econ Geol 27:344–364
Kuyunko NS, Semenov YV, Gurevich VM, Kuzmin VI, Topor ND, Gorbunov VE (1984) Experimental determination of thermodynamic properties of the tourmaline dravite. Geokhimiya 10:1458–1465 (in Russian)
LaPierre PT (1977) The geology, zoning, and textural features of the Second Pond ore deposit, Blue Hill, Maine. Unpub MS Thesis, Univ Maine, 75 pp
Lea ER, Dill DB (1968) Zinc deposits of the Balmat-Edwards district, New York. In: Ridge JD (ed) Ore Deposits of the United States, 1933–1967. The Graton-Sales Volume. Am Inst Min Metall Petr Eng 1:20–48
Lonsdale P, Becker K (1985) Hydrothermal plumes, hot springs, and conductive heat flow in the southern trough of Guaymas Basin. Earth Planet Sci Lett 73:211–225
Malinko SV, Lisitsyn AYe, Sumin LV (1982) Boron isotope distribution in natural borates and borosilicates as an indicator of conditions of their genesis. Dok Akad Nauk SSSR, Earth Sci Sec 267:193–195
Manning DAC (1981) The application of experimental studies in determining the origin of topaz-quartz-tourmaline rock and tourmaline-quartz rock. Proc Ussher Soc 5(2):121–127
Manning DAC, Pichavant M (1983) The role of fluorine and boron in the generation of granitic melts. In: Atherton MP, Gribble CD (eds) Migmatites, melting and metamorphism. Shiva Publishing Ltd., Nantwich, UK, pp 94–109
Mesmer RE, Baes CF Jr, Sweeton FH (1972) Acidity measurements at elevated temperatures. VI. Boric acid equilibria. Inorg Chem 11:537–543
Mielke H, Schreyer W (1969) Mineralparagenesen in Metasedimenten des Fichtelgebirges. Geol Bavaria 60:29–44
Miller RMcG (1983a) Tectonic implications of the contrasting geochemistry of Damaran mafic volcanic rocks, South West Africa/Namibia. In: Miller RMcG (ed) Evolution of the Damara orogen of South West Africa/Namibia. Geol Soc S Afr Spec Publ 11:115–138
Miller RMcG (1983b) The Pan-African Damara orogen of South West Africa/Namibia. In: Miller RMcG (ed) Evolution of the Damara orogen of South West Africa/Namibia. Geol Soc S Afr Spec Publ 11:431–515
Moine B, Sauvan P, Jarousse J (1981) Geochemistry of evaporite-bearing series: A tentative guide for the identification of metaevaporites. Contrib Mineral Petrol 76:401–412
Morey GB (1983) Animikie basin, Lake Superior region, U.S.A.: In: Trendall AF, Morris RC (eds) Iron-formation: Facts and problems. Elsevier, Amsterdam, pp 13–67
Musashi M, Nomura M, Okamoto M, Ossaka T, Oi T, Kakihana H (1988) Regional variation in the boron isotopic composition of hot spring waters from central Japan. Geochem J 22:205–214
Naqvi SM, Rogers JJW (1987) Precambrian geology of India. Oxford Univ Press, New York, 223 pp
Nash JT, Hahn GA (1989) Stratabound Co-Cu deposits and mafic volcaniclastic rocks in the Blackbird mining district, Lemhi County, Idaho. In: Boyle RW, Brown AC, Jefferson CW, Jowett EC, Kirkham RV (eds) Sediment-hosted stratiform copper deposits. Geol Assoc Can Spec Pap 36 (in press)
Nesbitt BE (1979) Regional metamorphism of the Ducktown, Tennessee, massive sulfides and adjoining portions of the southern Blue Ridge Province. Unpub PhD Thesis, Univ Michigan, 238 pp
Nesbitt BE, Longstaffe FJ, Shaw DR, Muehlenbachs K (1984) Oxygen isotope geochemistry of the Sullivan massive sulfide deposit, Kimberley, British Columbia. Econ Geol 79:933–946
Nicholson PM (1980) The geology and economic significance of the Golden Dyke dome, Northern Territory. In: Ferguson J, Goleby AB (eds) Uranium in the Pine Creek Geosyncline. Internat Atomic Energy Agency, Vienna, pp 319–334
Norton JJ (1976) Field compilation map of the geology of the Keystone area, Black Hills, South Dakota. US Geol Surv Open-File Map 76–297, scale 1:24000
Palache C (1935) The minerals of Franklin and Sterling Hill, N.J. US Geol Surv Prof Paper 180, 135 pp
Palmer MR, Spivack AJ, Edmond JM (1987) Temperature and pH controls over isotopic fractionation during adsorption of boron on marine clay. Geochim Cosmochim Acta 51:2319–2323
Pavlides L, Gair JE, Cranford SL (1982) Central Virginia volcanic-plutonic belt as a host for massive sulfide deposits. Econ Geol 77:233–272
Phillips GN (1980) Water activity across an amphibolite-granulite facies transition, Broken Hill, Australia. Contrib Mineral Petrol 75:377–386
Plimer IR (1983) The association of tourmaline-bearing rocks with mineralisation at Broken Hill, NSW. Austral Inst Min Metall Conf, Broken Hill, N.S.W., July, 1983, pp 157–176
Plimer IR (1985) Broken Hill Pb–Zn–Ag deposit –A product of mantle metasomatism. Mineral Deposita 20:147–153
Plimer IR (1986) Tourmalinites from the Golden Dyke dome, northern Australia. Mineral Deposita 21:225–239
Plimer IR (1988) Tourmalinites associated with Australian Proterozoic submarine exhalative ores. In: Friedrich GH, Herzig PM (eds) Base metal sulfide deposits in sedimentary and volcanic environments. Springer-Verlag, Berlin Heidelberg New York, pp 255–283
Plimer IR, Lees TC (1988) Tourmaline-rich rocks associated with the submarine hydrothermal Rosebery Zn–Pb–Cu–Ag–Au deposit and granites in western Tasmania, Australia. Mineral Petrol 38:81–103
Porada H, Behr HJ (1988) Setting and sedimentary facies of Late Proterozoic alkali lake (playa) deposits in the southern Damara belt of Namibia. Sediment Geol 58:171–194
Porada H, Wittig R (1983) Turbidites and their significance for the geosynclinal evolution of the Damara orogen of South West Africa/Namibia. In: Miller RMcG (ed) Evolution of the Damara orogen of South West Africa/Namibia. Geol Soc S Afr Spec Pub 11, 21–36
Preussinger H (1987) Die geologische Situation der Erzlinse Vendome, Gorob Bezirk, SWA/Namibia. Unpub MSc Thesis, Univ Würzburg, 131 pp
Ramberg IB (1967) Kongsfjell-omradets geologi, en petrografisk og strukturell undersokelse i Helgeland, Nord-Norge. Norge Geol Undersok 240, 152 pp
Rauhamaki E, Makela T, Isomaki O-P (1978) Geology of the Vihanti mine. In: Metallogeny of the Precambrian. Helsinki Acad Finland (Excursion Guide), pp 35–56
Raymond WH (1981) Geochemical data from Precambrian metairon-formation and related rocks of the Keystone area, South Dakota. US Geol Surv Open-File Rep 81–772, 13 pp
Rehtijarvi P, Aikas O, Makela M (1979) A Middle Precambrian uranium- and apatite-bearing horizon associated with the Vihanti zinc ore deposit, western Finland, Econ Geol 74:1102–1117
Rickard DT, Zweifel H (1975) Genesis of Precambrian sulfide ores, Skellefte district, Sweden. Econ Geol 70:255–274
Riesmeyer WD (1978) Precambrian geology and ore deposits of the Pecos mining district, San Miguel and Santa Fe Counties, New Mexico. Unpub MS Thesis, Univ New Mexico, 215 pp
Robbins CR, Yoder HS Jr (1962) Stability relations of dravite, a tourmaline. Carnegie Inst Wash Yearb 61:106–107
Robertson JM, Moench RH (1979) The Pecos greenstone belt: A Proterozoic volcano-sedimentary sequence in the southern Sangre de Cristo Mountains, New Mexico. In: Ingersoll RV (ed) Guidebook of Santa Fe Country. N M Geol Soc Field Conf Guideb 30:165–173
Ryan PJ, Lawrence AL, Lipson RD, Moore JM, Paterson A, Sted-

man DP, Van Zyl D (1986) The Aggeneys base metal sulphide deposits, Namaqualand, South Africa. In: Anhaeusser CR, Maske S (eds) Mineral deposits of southern Africa. Geol Soc S Afr II:1447–1474
Sangster DF (1988) Relative sulphur isotope abundances of ancient seas and stratabound sulphide deposits. Geol Assoc Can Proc 17:79–91
Schalk KEL (1988) Geological map 22117 DC-Dordabis. Geol Surv S West Afr/Namibia, scale 1:50000 (unpub)
Schmidt RG (1963) Geology and ore deposits of the Cuyuna North Range, Minnesota. US Geol Surv Prof Paper 407, 96 pp
Schreyer W, Abraham K (1976) Three-stage metamorphic history of a whiteschist from Sar e Sang, Afghanistan, as part of a former evaporite deposit. Contrib Mineral Petrol 59:111–130
Shaw DM, Truscott MG, Gray EA, Middleton TA (1988) Boron and lithium in high-grade rocks and minerals from the Wawa-Kapuskasing region, Ontario. Can J Earth Sci 25:1485–1502
Shima M (1963) Boron isotope ratio on some Japanese boron minerals. Tokyo Inst Phys Res Rpts 39:207–210 (in Japanese)
Sisson VB, Closmann CE, Leeman WP, Truscott MG, Holdaway MJ (1988) Boron loss during low pressure progressive metamorphism of central Maine and southern Chugach Mountains, Alaska. Geol Soc Am Abs Pgms 20:A342
Slack JF (1980) Tourmaline – A prospecting guide for massive base-metal sulfide deposits in the Penobscot Bay area, Maine. Maine Geol Surv Spec Econ Stud Ser 8, 25 pp
Slack JF (1982) Tourmaline in Appalachian-Caledonian massive sulphide deposits and its exploration significance. Trans Inst Mining Metall 91(B):B81–89
Slack JF, Coad PR (1989) Multiple hydrothermal and metamorphic events in the Kidd Creek volcanogenic massive sulphide deposit, Timmins, Ontario: Evidence from tourmalines and chlorites. Can J Earth Sci 26:694–715
Slack JF, Godchaux MM, Graves RL (1983) Volcanogenic massive sulphide deposits of the Davis mine, Hampshire County, Massachusetts. In: Sangster DF (ed) Field trip guidebook to stratabound sulphide deposits, Bathurst area, N.B., Canada and west-central New England, U.S.A. Geol Surv Can Misc Rep 36:53–63
Slack JF, Herriman N, Barnes RG, Plimer IR (1984) Stratiform tourmalinites in metamorphic terranes and their geologic significance. Geology 12:713–716
Slack JF, Palmer MR, Edmond JM (1987) A boron isotope study of the Broken Hill district, Australia. Geol Soc Am Abs Pgms 19:847
Slater R (1982) Massive sulfide deposits of the Ducktown mining district, Tennessee. In: Allard GO, Carpenter RH (eds) Exploration for metallic resources in the Southeast. Dept Geology, Univ Georgia, pp 91–99
Smith JV, Brown WL (1988) Feldspar minerals, vol 1, crystal structures, physical, chemical, and microtextural properties. Springer-Verlag, Berlin Heidelberg New York, 828 pp
Solomon M, Vokes FM, Walshe JL (1987) Chemical remobilization of volcanic-hosted sulphide deposits at Rosebery and Mt. Lyell, Tasmania. Ore Geol Rev 2:173–190
Spivack AJ (1986) Boron isotope geochemistry. Unpub PhD Thesis. MIT-WHOI Joint Prog Oceanogr, 184 pp
Spivack AJ, Edmond JM (1986) Determination of boron isotope ratios by thermal ionization mass spectrometry of the dicesium metaborate cation. Anal Chem 58:31–35
Spivack AJ, Edmond JM (1987) Boron isotope exchange between seawater and the oceanic crust. Geochim Cosmochim Acta 51:1033–1043
Spivack AJ, Palmer MR, Edmond JM (1987) The sedimentary cycle of the boron isotopes. Geochim Cosmochim Acta 51:1939–1949
Stametelopoulou-Seymour K, MacLean WH (1984) Metamorphosed volcanogenic ores at Montauban, Grenville Province, Quebec. Can Mineral 22:595–604
Stanton RL (1972) A preliminary account of chemical relationships between sulfide lode and "banded iron formation" at Broken Hill, New South Wales. Econ Geol 67:1128–1145
Stevens BPJ (1986) Post-depositional history of the Willyama Supergroup in the Broken Hill block, NSW. Aust J Earth Sci 33:73–98
Stevens BPJ, Barnes RG, Brown RE, Stroud WJ, Willis IL (1988) The Willyama Supergroup in the Broken Hill and Euriowie blocks, New South Wales. Precam Res 40/41:297–327
Swihart GH, Moore PB (1989) A reconnaissance of the boron isotopic composition of tourmaline. Geochim Cosmochim Acta 53:911–916
Swihart GH, Moore PB, Callis EL (1986) Boron isotopic composition of marine and nonmarine evaporite borates. Geochim Cosmochim Acta 50:1297–1301
Swinden HS, Jenner GA, Kean BF, Evans DTW (1989) Volcanic rock chemistry as a guide for massive sulphide exploration in central Newfoundland. Nfld Dept Mines Energy, Curr Res Rep 89-1:201–219
Takeda H (1970) Structural study on the stratified pyrite deposits in the Shirataki and Sazare mining district, Shikoku. In: Tatsumi T (ed) Volcanism and ore genesis. Univ Tokyo Press, pp 77–91
Tanner PWG (1972) Regional correlation and stratigraphic position of the host rocks to the Kilembe ore body, Uganda. Research Unit African Geol, Univ Leeds, 16th Ann Rep, pp 24–28
Taylor BE, Slack JF (1984) Tourmalines from Appalachian-Caledonian massive sulfide deposits: Textural, chemical, and isotopic relationships. Econ Geol 79:1703–1726
Taylor HP Jr (1974) The application of oxygen and hydrogen isotope studies to problems of hydrothermal alteration and ore deposition. Econ Geol 69:843–883
Theart HFJ, Cornell DH, Schade J (1989) Geochemistry and metamorphism of the Prieska Zn–Cu deposit, South Africa. Econ Geol 84:34–48
Truscott MG, Percival JA (1988) The boron cycle in metasedimentary rocks and derived granite, Quetico belt, Ontario. Geol Assoc Canada, Pgms Abs 13:A126–A127
Tuach J (1984) Geology and sulfide mineralization in the Rambler area, Newfoundland – A 1984 perspective. Nfld Dept Mines Energy, Curr Res Rep 84-3:91–97
Tuach J, Kennedy MJ (1978) The geologic setting of the Ming and other sulfide deposits, Consolidated Rambler mines, northwest Newfoundland. Econ Geol 73:192–206
Uhlig SH (1987) Die oberproterozoische Duruchaus Formation in Namibia und ihre Kupfervererzungen. Unpub DSc Thesis, Univ Giessen, 163 pp
Vokes FM (1963) Geological studies on the Caledonian pyritic zinc-lead orebody at Bleikvassli, Nordland, Norway. Norges Geol Undersok 222, 126 pp
Von Damm KL, Edmond JM, Measures CI, Grant B (1985a) Chemistry of submarine hydrothermal solutions at Guaymas Basin, Gulf of California. Geochim Cosmochim Acta 49:2221–2237
Von Damm KL, Edmond JM, Grant B, Measures CI, Walden B, Weiss RF (1985b) Chemistry of submarine hydrothermal solutions at 21° N, East Pacific Rise. Geochim Cosmochim Acta 49:2197–2220
Wagener JHF, van Schalkwyk I (1986) The Prieska zinc-copper deposit, northwest Cape Province. In: Anhaeusser CR, Maske S (eds) Mineral deposits of southern Africa. Geol Soc S Afr II:1503–1528
Walker RR, Matulich A, Amos AC, Watkins JJ, Mannard GW (1975) The geology of the Kidd Creek mine. Econ Geol 70:80–89
Warden AJ (1985) Reappraisal of geological setting and potential of Kilembe copper mine, Uganda. Trans Inst Mining Metall 94(B):B94–B105
Werding G, Schreyer W (1984) Alkali-free tourmaline in the system $MgO-Al_2O_3-B_2O_3-SiO_2-H_2O$. Geochim Cosmochim Acta 48:1331–1344

White WS, Eric JH (1944) Preliminary report on the geology of the Orange County copper district, Vermont. US Geol Surv Open-File Rep, 36 pp

Willden M (1986) Geology of the western part of the Skellefte field and the Kristineberg and Hornträsk sulphide deposits. In: Rickard D (ed) The Skellefte Field. Sveriges Geol Undersok, NR 62 (7th IAGOD Symp, Excur Guide 4), pp 46–54

Willis IL, Brown RE, Stroud WJ, Stevens BPJ (1983) The Early Proterozoic Willyama Supergroup: Stratigraphic subdivision and interpretation of high to low-grade metamorphic rocks of the Broken Hill block, New South Wales. J Geol Soc Aust 30:195–224

Wright JV, Haydon RC, McConachy GW (1987) Sedimentary model for the giant Broken Hill Pb–Zn deposit, Australia. Geology 15:598–602

Received January 22, 1989 / accepted July 10, 1989
Editorial responsibility: W. Schreyer